AN ABSTRACT OF THE THESIS OF

Heather M. Baron for the degree of Master of Science in Marine Resource Management presented on June 2, 2011.

Title: Coastal Hazards and Community Exposure in a Changing Climate: The Development of Probabilistic Coastal Change Hazard Zones.

Abstract approved:

_____

Peter Ruggiero

Documented trends in rising sea levels, storminess, and extreme wave heights have the potential to increase the frequency and magnitude of coastal change hazards, increasing risks to coastal infrastructure and environmental resources. Coastal planners and decision makers need information about the impacts of future hazards in order to apply mitigation and adaptation strategies. However, making quantitative predictions of beach and dune erosion is complicated by uncertainties surrounding the drivers and impacts of climate change as well as our understanding of climate controls on coastal change hazards. Furthermore, these changes are occurring in a dynamic environment where beach geomorphology evolves over a variety of spatial and temporal scales. Here a new, probabilistic approach for quantifying future coastal change hazards that incorporates the uncertainty associated with both climate change and morphological variability is presented.

First, a suite of synthetic time series of total water levels (TWLs) through 2100 are produced by applying various climate change scenarios, composed of projections of sea-level rise, wave climate, and the frequency of major El Niños, to historical datasets of waves and measured tidal elevations. These time series allow extreme design events to be computed for any time period in the future (e.g., 100-year TWL event in 2030). Using simple coastal change models that require TWLs and various beach morphometrics as input, future coastal change is quantified over a wide range of possible climate futures for sandy, dune-backed coastlines.

The new methodology has been applied to the Tillamook County coast in northwestern Oregon to develop coastal change hazard zones of arbitrary confidence levels for both the 100% and 1% annual chance TWL events at present (2009) and for years 2030, 2050, and 2100. The nature of the probabilistic approach, however, allows for coastal decision makers to determine the desired level of confidence (or exceedance probability), extremity of the event, and planning horizon to consider. The hazard zones are then integrated with various socioeconomic datasets (e.g., structures, roads) to evaluate the exposure of coastal communities to the predicted coastal change hazards at various levels of confidence. When paired with community vulnerability assessments, the hazard map products developed will provide coastal planners with the tools and information to allow for science-based decisions that will increase the adaptive capacity of coastal communities as they prepare for the uncertainties of future climate change.

Coastal Hazards and Community Exposure in a Changing Climate: The Development of Probabilistic Coastal Change Hazard Zones

by
Heather M. Baron

A THESIS

submitted to

Oregon State University

in partial fulfillment of
the requirements for the
degree of

Master of Science

Presented June 2, 2011
Commencement June 2012

Master of Science thesis of Heather M. Baron presented on June 2, 2011.

APPROVED:

_____

Major Professor, representing Marine Resource Management

_____

Dean of the College of Oceanic and Atmospheric Sciences

_____

Dean of the Graduate School

I understand that my thesis will become part of the permanent collection of Oregon State University libraries. My signature below authorizes release of my thesis to any reader upon request.

_____

Heather M. Baron, Author

ACKNOWLEDGEMENTS

I would first like to thank my advisor, Peter Ruggiero, for providing me the opportunity to work on this research. From the beginning, your passion for coastal science has been contagious. Your guidance and involvement over the years has helped me grow as a scientist. I am truly grateful to have had such a great mentor who challenged me and encouraged me the way that you did.

To my other committee members, Nate Wood and Dawn Wright – it has been a pleasure learning from both of you. I know I would not have nearly the same amount of GIS skills as I do now had it not been for your teaching and assistance. I would also like to thank Jonathan Allan, Paul Komar, and Pat Corcoran. All three of you have acted as additional committee members and mentors to me. I appreciate your input and encouragement, and I have enjoyed working with you all.

Thank you to the Neskowin Coastal Hazards Committee for letting me sit in on meetings and be a part of your planning process. I hope your efforts help bring awareness to the community to protect it for future generations. A special thanks to Mitch Rohse and Laren Woolley for the countless conference calls and email conversations we've had to help us figure out the best way to present our hazard map products. I am delighted that you have chosen to include our research in the Tillamook County Erosion Hazards Adaptation Framework Plan and Neskowin Sub-Plan.

I would like to thank all the members of the CIL for being such great officemates, not letting me lose my mind as I struggled to learn Matlab, and for the endless supply of chocolate (John). Thank you also to my fellow MRMers, especially Joy Irby, my partner

throughout the madness of Salmon Bowl – what a whirlwind of a first year that was! And, of course, thanks to the original Nearshore All-Stars: Erica Harris, Jeremy Mull, Justin Brodersen, Katy Serafin, Diana DiLeonardo, and Jeff Wood. My time here would not have been as enjoyable without you or Guns and Roses. I would also like to thank vital members of the COAS family without whom I may never have come to OSU – Robert Allan, Lori Hartline, and Bob Duncan. Ever since your warm welcome on my first visit to Corvallis during Open House, you have provided me with endless advice, assistance, and support that has been both helpful and comforting. Thank you also to my family and closest friends who have supported me in all my endeavors. I know it's been a long, and sometimes, quite difficult journey, but I promise I'll be out of school one day soon!

Last but not least, this work would not have been possible without the funding support provided by the Sectoral Applications Research Program (SARP) of the National Oceanic and Atmospheric Administration's Climate Program Office under NOAA Grant# NA08OAR4310693 or the GIS data provided to us by the folks at the Tillamook County Community Development and Assessment & Taxation departments. Thank you.

TABLE OF CONTENTS

LIST OF FIGURES

Figure Page

LIST OF FIGURES (Continued)

Figure Page

LIST OF TABLES

Coastal Hazards and Community Exposure in a Changing Climate: The Development of Probabilistic Coastal Change Hazard Zones

1. INTRODUCTION

The coast of the U.S. Pacific Northwest (PNW) is a highly dynamic environment that responds over a variety of spatial and temporal scales to external forcings, such as wave energy, fluctuations in water levels, or gradients in longshore sediment transport, through the erosion and accretion of the shoreline. While the wave climate in the PNW is known for its severity year-round, the largest storm events typically occur during the winter, often resulting in the episodic erosion of coastal foredunes (Komar et al., 1999). Furthermore, when severe storms coincide with periods of elevated water levels (e.g., during spring tides or El Niño events), the threat of significant coastal erosion, as well as dune overtopping, is increased (Allan and Komar, 2006). Because these natural processes are occurring in places where people live, work, and recreate, they represent a potential harm to both social and ecological systems and can therefore be defined as hazards.

The Earth's variable and changing climate directly influences the physical processes driving the erosion of beaches and properties of the West Coast (Allan and Komar, 2006). Documented trends in rising sea levels (e.g., Church and White, 2006), storminess (e.g., Graham and Diaz, 2001), and extreme wave heights (e.g., Ruggiero et al., 2010) have the potential to increase the frequency and magnitude of coastal change hazards in the PNW, increasing risk to coastal infrastructure and environmental resources. Further, as coastal populations rise and development pressures increase, there

will be more and more valuable assets located in hazardous regions (Crossett et al., 2004). The impacts of climate change to oceanfront communities will significantly depend on land use patterns along the coast, necessitating place-based analyses to determine the vulnerability of these communities to the evolving magnitudes and frequency of physical hazards. Here vulnerability is characterized by quantifying the potential magnitude of coastal change likely to be experienced and the exposure of valuable oceanfront property to those hazards.

Making quantitative predictions of future coastal change hazards, however, is complicated by uncertainties and knowledge gaps surrounding the drivers of climate change, the magnitude of its impacts, the complexity of coastal systems, and our understanding of climate controls on coastal change hazards. Nevertheless, coastal planners and emergency managers require information about the potential impacts of climate change to develop long-term adaptation strategies. It is within this context of uncertainty and societal need that new methodologies for predicting future coastal change hazards have been developed and are presented here, in order to perform assessments of the exposure and vulnerability of communities and oceanfront properties.

1.1 Approaches for Characterizing Coastal Vulnerability

Various approaches exist for predicting and communicating potential impacts to coastal areas due to climate change and/or extreme events. One method is a qualitative approach that relies on the development of physically-based indices to describe the relative vulnerability of coastlines through the development of, for example, a Coastal

Vulnerability Index (CVI) (e.g., Gornitz et al., 1997; Thieler and Hammar-Klose, 1999). This approach involves the ranking of various geologic and environmental variables that influence a coastline's vulnerability, such as rate of relative sea-level rise (SLR), regional beach slope, shoreline change rates, tidal range, and mean wave height. The CVI is useful in that it can be computed over a large area (regional to national scale) with diverse geomorphology without needing detailed input data to drive physical models. Several coastlines around the world have been characterized using CVIs, for example, the United States (Hammar-Klose and Thieler, 2001), Canada (Shaw et al., 1998), and India (Kumar et al., 2010). The CVI, however, only identifies areas that are relatively more vulnerable than others, rather than estimating the expected magnitude of coastal change or inundation that may result from a prescribed amount of SLR.

Other methods are more quantitative in their assessment of coastal hazards. Most common is the event-selection, or benchmark event, approach that simply involves selecting various forcing parameters (e.g., wave height, water level) that can combine to approximate a particular design event of interest (e.g., 100-year total water level). This method, for example, is used for existing coastal change hazard zones in Oregon (Allan and Priest, 2001). The zones are developed deterministically by calculating the magnitude of erosion likely to occur due to a specific significant storm event (typically the largest on historical record) during an above-average high tide. Because this approach is based on a single event, it results in a single estimation of expected erosion rather than some probability of occurrence. In addition, this approach often excludes the fact that beaches are constantly changing and evolving over a variety of timescales, and

climate change can only be incorporated in a fairly ad hoc manner without a detailed exploration of the possible parameter space.

Another, more statistical method is the response-based, or structural function, approach where relevant parameters are combined to determine some variable of interest. For example, data quantifying measured waves and water levels could be used to estimate potential beach erosion or flooding extent using various physical models. Work by Philip Williams & Associates (PWA, 2009; Revell et al., in press) aims to quantify the impacts of SLR on the coast of California through the use of total water level (TWL) exceedance curves, where a relationship between the current position of the dune toe and TWL is determined and then used to quantify future coastal change based on changing water levels. Their methods involve the development of a limited number of TWL time series through 2100, using output from a global climate model, for two separate sea-level rise (SLR) scenarios.

Most complete are fully probabilistic, full temporal simulation approaches that account for dependencies between all relevant variables. Full simulation approaches (e.g., Callaghan et al., 2008) involve randomly sampling, in a Monte Carlo sense, from fitted probability distributions that represent the important variables and their dependencies. Both the response-function and full simulation approaches have the potential to include the non-stationarity associated with climate change; the methodology presented here is based on the former of the two.

It is recognized that vulnerability is not only a function of potential physical impacts, but also requires some understanding of the socioeconomic dimension;

therefore, it is important to examine the amount of assets likely to be affected (exposure), the impact those losses may have on the community as a whole (sensitivity), and how equipped the community is to respond and adapt (resilience; e.g., Turner et al., 2003; Adger, 2006). Despite this, less work has been done on relating potential coastal hazards to the human-environmental systems they may be impacting. Boruff et al. (2005) combine a socioeconomic vulnerability index (SoVI) with the CVI developed by the U.S. Geological Survey (USGS) for the Atlantic, Pacific, and Gulf of Mexico coasts (e.g., Hammar-Klose and Thieler, 2001) to produce an index for the overall place vulnerability of each U.S. coastal county that is characterized by various social, economic, and physical factors. The SoVI is constructed using data from the U.S. Census for coastal counties such as poverty, age, development density, income, and race, among others. In all, 39 variables were considered but only 10 were sufficient to explain 82% of the variance among counties. These factors were combined additively (no weighting was assigned) to determine the relative vulnerability of each county. Counties with the highest vulnerability ranking on the West Coast were highly populated areas of California and along the Puget Sound in Washington. The Oregon coast was ranked as having relatively low to medium vulnerability because there is less ethnic diversity and low levels of urban development.

After the California coastal erosion assessment by PWA, the Pacific Institute (Heberger et al., 2009) performed an analysis of the current population, infrastructure, and property at risk to future SLR if no protective actions were taken and developed recommended practices and policies for the state to consider based on their findings.

They found that a SLR of 1.4 m by 2100 would put 480,000 people and a wide range of critical infrastructure at risk to a major flood event. In addition, some areas of the California coast that were not particularly vulnerable to flooding were highly susceptible to erosion. It was recommended that development along the coast of California be limited in the future to reduce risks to both of these coastal hazards.

While no such work has yet to be performed on the Oregon coast, the USGS has conducted a study of the Oregon coast to examine the exposure and sensitivity of coastal communities to tsunami hazards (Wood, 2007). This work shows that vulnerability varies considerably among the coastal communities of Oregon, and is primarily determined by how communities occupy and use tsunami-prone land. Some cities have a high amount of assets in the tsunami-prone land (high exposure) that represent a low percentage of the total assets in the city (low sensitivity). Others have a relatively small amount of exposed assets but these represented a large percentage of the city's total assets, making them more highly sensitive to tsunami hazards.

1.2 Objectives

The research described in this thesis is part of a larger effort examining the role of climate change and variability in the erosion of the U.S. West Coast, funded by NOAA's Climate Program Office Sectoral Applications Research Program. The goals of the overall study are to improve understanding of climate controls on coastal hazards (e.g., waves, storm surges, mean sea level), enhance coastal hazard models to incorporate

climate controls, assess societal vulnerability to potential coastal change hazards, and then develop tools to support coastal resource, land use, and emergency managers.

The primary aim of the research presented here is to develop a probabilistic methodology to quantify future coastal change hazards that incorporates the uncertainty associated with climate change and variability in order to begin to assess the vulnerability of coastal communities to these hazards. The following specific objectives contribute to meeting this goal:

1. Develop a suite of climate change scenarios that incorporate the uncertainty associated with future water levels (e.g., sea-level rise, storminess, and major El Niño occurrences);
2. Through the use of simple models, quantify potential coastal change hazards and generate a series of probabilistic hazard zones for select events at various time frames in the future that account for both climate and morphological uncertainty; and
3. Integrate these hazard zones with local socioeconomic data to assess the exposure of oceanfront communities to future coastal change hazards.

The nature of the probabilistic approach allows for coastal decision makers to determine the extremity of the event and planning horizon to consider, as well as the desired level of confidence (or exceedance probability) they would like to plan for. The coastal change hazard zones developed can then be disseminated to local planning groups as maps or digital data layers. Paired with community vulnerability assessments, these hazard map products provide coastal planners with the necessary tools and information to

allow for science-based decisions that will increase the adaptive capacity of coastal communities as they prepare for the uncertainties of future climate change. In addition, by developing a probabilistic approach, the relative role of climate-change related factors and morphological variability on erosion hazards can be explored.

2. STUDY AREA

The Oregon coast is composed of a mixture of sandy beaches and rocky shores, which have been shaped by various geologic and oceanographic processes over millions of years. Large, erosion-resistant headlands separate the coast into a series of self-contained littoral cells, with limited or no sand exchange between them (Komar, 1998). Beaches within these littoral cells range from highly dissipative with fine sands, low slopes, and wide surf zones to reflective, characterized by much steeper slopes, coarser grain sizes, and a narrow beach and surf zone (Wright and Short, 1983). In the summer, waves generally approach the coast from the northwest, moving sediment towards the southern end of these littoral cells. During the winter months, sediment is moved to the north by waves approaching out of the southwest. This seasonality in the incident wave approach angles is typically thought to result in no significant net littoral drift of sediment along the coast (Komar, 1998).

During the summer, monthly mean significant wave heights are on the order of 1.5 m with periods of ~8 s, while wave heights in the winter are typically double in height, averaging ~3 m with periods on the order of 12-13 s (Ruggiero et al., 2005). Winter storms in the region annually generate wave heights greater than 10 m, while some of the strongest storms on record have generated waves up to as much as 14 m (Allan and Komar, 2002; 2006). Peak periods associated with these large wave heights tend to be about 15-17 s, but can be as large as 20 s (Allan and Komar, 2002).

The PNW experiences mixed semidiurnal tides with an average tidal range on the order of 2 m and a maximum range of about 4 m (Komar, 1998). Water levels are

highest during the winter months due to thermal expansion of the warm surface water that is flowing northward and being piled up at the shore by the earth's Coriolis force (Komar, 1998). Strong, onshore winds and low atmospheric pressures during winter storms can also raise water levels as storm surges. During an extreme storm that occurred on 2-4 March 1999, surges on the order of 1-1.5 m were measured along the Oregon and Washington coasts (Allan and Komar, 2002). Storm surges in the PNW are not nearly as large as those on the East Coast where the continental shelf is much wider, though they can be an important component to consider when estimating potential coastal change.

The Oregon coast is also affected by large-scale climate variations such as the El Niño/La Niña-Southern Oscillation (ENSO). During the warm phase of this cycle, or El Niño, water levels along the U.S. West Coast are typically raised by tens of centimeters (Allan and Komar, 2006). In addition, anomalous wave approach angles and larger than typical wave heights act to enhance longshore sediment transport causing hotspot erosion at the southern ends of some littoral cells (e.g., Komar, 1986; Kaminsky et al., 1998; Allan and Komar, 2006). While ENSO events typically occur every 3-5 years and last from 6 to 18 months, these cycles are superimposed on larger patterns of climate variability known as the Pacific Decadal Oscillation (PDO). The PDO is a low frequency modulation of ENSO variability with cycles persisting for 20-30 years. Since about the mid-1970s, the PDO has been in a warm phase with more El Niño-like conditions occurring over the last few decades; however, there is recent evidence to suggest that we are now in a cool phase, more La Niña-like, which could act to suppress coastal

upwelling, leaving surface waters warmer and raising sea level on the West Coast (Bromirski et al., in press).

The focus here is on the Tillamook County coast located in northwest Oregon, though the methodology is applicable to all dune-backed stretches of shoreline in the Pacific Northwest. The littoral cells of Tillamook County and their major bounding headlands (pictured in Figure 1), include: Rockaway (Cape Falcon to Cape Meares), Netarts (Cape Meares to Cape Lookout), Sand Lake (Cape Lookout to Cape Kiwanda), and Neskowin (Cape Kiwanda to Cascade Head). Each littoral cell is further divided by at least one estuary, two of which have inlets stabilized by jetties (Tillamook Bay and Nehalem Bay). The mouths of the other estuaries are free to migrate and shift in response to various hydrodynamic forcings, as the sediment budget allows. The Rockaway littoral cell is the largest and most densely populated of the Tillamook County coast, with over six distinct communities located along 25 km of shoreline. The central portion of this littoral cell, Rockaway Beach, is the main site for commercial development and tourist accommodations.

There are two communities at the northern end of the Netarts littoral cell (Oceanside and Netarts), but neither of these are located along dune-backed beaches; therefore, the focus in this cell is the 7.5 km-long Netarts Spit (the site of Cape Lookout State Park – a popular recreation spot for both tourists and local residents), which has been experiencing significant dune erosion and overtopping over the last few decades (Allan and Komar, 2004). As a result, a dynamic cobble revetment lines the shore of the southern portion of the littoral cell near the State Park's campground.

The Sand Lake littoral cell is also largely uninhabited. Beaches along both the northern and southern ends of the littoral cell are backed by coastal bluffs. The dune-backed shoreline is located on other side of Sand Lake, stretching about 6 km. South of Sand Lake is the unincorporated community of Tierra Del Mar, only ~0.2 km^2 in size.

Furthest south is the Neskowin littoral cell. While the northern part of this littoral cell has been experiencing an influx of sediment over the last few decades, covering parking lots, roads, and accumulating in and around houses in Pacific City, there has been significant erosion occurring in the southern part, threatening oceanfront residences in Neskowin. This small community of less than 200 residents is presently situated behind a continuous stretch of riprap which serves as a barrier between the destructive power of storm waves and valuable property. The growing concern of community members has prompted the development of the Neskowin Coastal Hazards Committee, which consists of local residents and representatives from various state agencies (e.g., the Oregon Department of Land Conservation and Development, the Oregon Parks and Recreation Department, and the Tillamook County Planning Commission), whose focus is to maintain and preserve their beach as well as protect their community. This local activism has sparked both community and county-wide interest in planning for future erosion hazards.

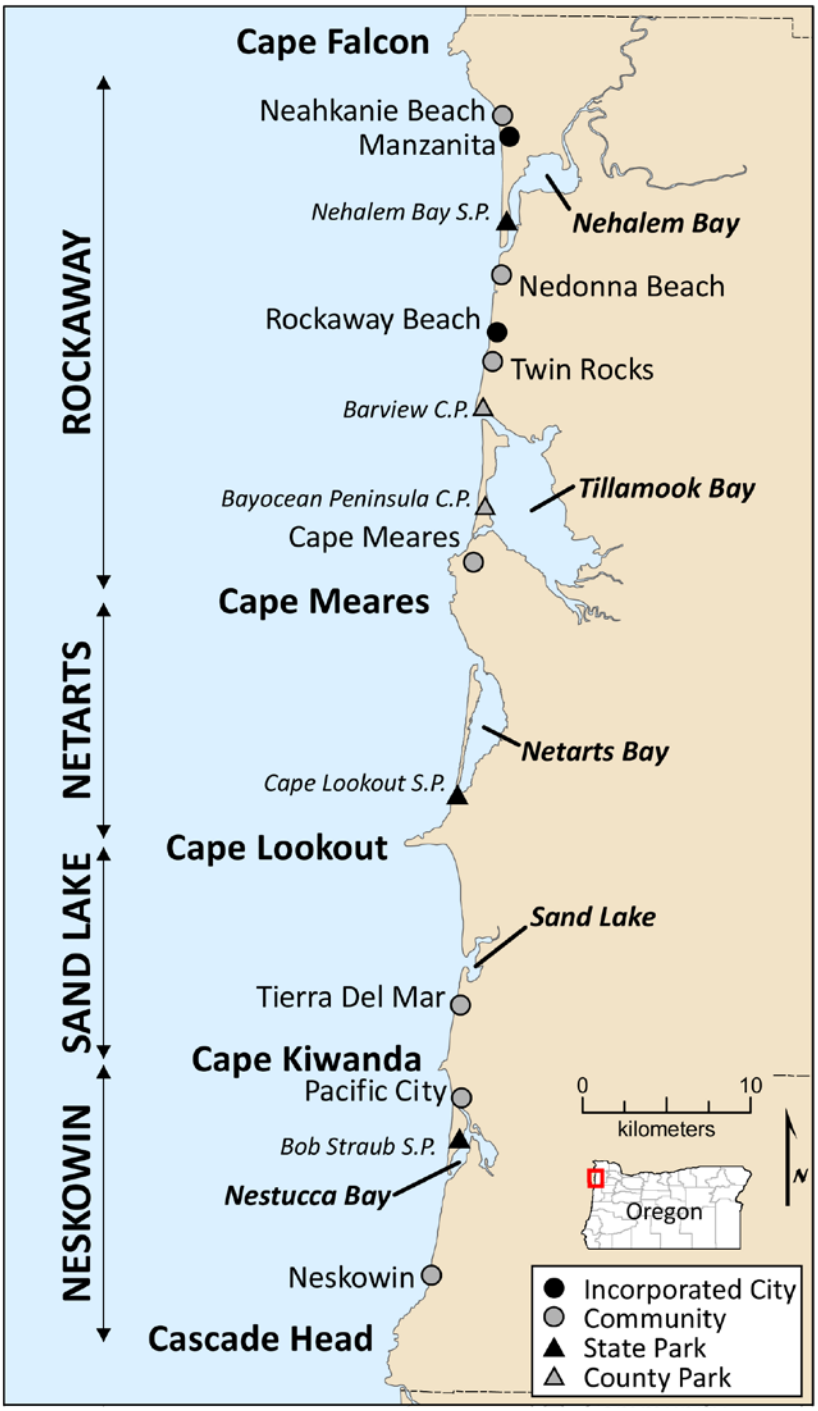

Figure 1. Map of the four littoral cells of Tillamook County, as divided by five major headlands, showing the coastal communities, estuaries, and recreational parks along the coast.

3. METHODS

In order to quantify coastal change hazards and subsequently evaluate community exposure, a probabilistic approach that incorporates climate change and morphological uncertainty has been developed. Below, first is a description of how a coastal change hazard zone is defined. This is followed by a discussion of the climate change scenario development, highlighting each of the three components considered. Next is a detailed look at the erosion models used in deriving the hazard zones as well as the morphometric and hydrodynamic inputs needed to apply the models. This section concludes with a brief discussion of how predicted coastal change hazards are integrated with socioeconomic datasets to perform exposure analyses of coastal communities.

3.1 Defining Coastal Change Hazard Zones

To evaluate exposure to coastal change hazards, zones are developed that identify where coastal change associated with particular design events (e.g., 1% and 100% annual chance events) is likely to occur at various planning horizons (e.g., present-day, 2030, 2050, 2100) for a desired level of confidence or exceedance probability (e.g., 2%, 50%, 98%). A general expression for a coastal change hazard zone (CCHZ) can be written as

$$CCHZ = (CCR_{SB} + CCR_{climate})T + CC_{event} + CC_{HS} \quad (1)$$

where CCR_{SB} and $CCR_{climate}$ are the coastal change rates associated with trends in sediment budgets and climate change-induced factors (e.g., rising sea levels, storm surge trends), respectively. These two components are multiplied by T, the time period of interest for the CCHZ. This can be on the order of several years to decades but the

uncertainty in the model results increases as projections are made further into the future. Since significant erosion often occurs episodically during large storms, to fully examine the physical susceptibility of the coast necessitates the term CC_{event}, the coastal change associated with an extreme elevated water level event, such as the annual or 100-year event, which, respectively, have a 100% and 1% chance of occurring in any given year. Conservatism is built into the approach by adding this term to the CCHZ after both CCR_{SB} and $CCR_{climate}$ have acted on the coast for the full time period of interest. Finally, CC_{HS} is a parameter that can be included to account for coastal change associated with erosion hotspots that may develop during El Niños or localized scour due to rip currents.

For the application described here, the terms CCR_{SB} and CC_{HS} in Equation 1 are not directly modeled as these are typically poorly known and difficult to project into the future, especially when a quantified sediment budget is not readily available. However, an effort to account for coastal change resulting from these two processes is achieved through other ways in the methodology (e.g., incorporating morphological variability and choosing conservative confidence levels). For the remaining terms, $CCR_{climate}$ and CC_{event}, simple geometric models are used to estimate the maximum potential erosion that could occur under a variety of different climate change scenarios. $CCR_{climate}$ is calculated using the Bruun Rule (Bruun, 1962; 1988) to estimate the landward retreat of the coast due to sea-level rise. The dune erosion model of Komar et al. (1999), hereinafter referred to as K99, is used to calculate CC_{event}, which predicts retreat of the foredune when the TWL exceeds the elevation of the beach-dune junction, or dune toe. While the models applied here are simple, the modular design of the approach allows for more sophisticated

models to be used when more details are desired and the necessary input data are available.

3.2 Developing Climate Change Scenarios

Predicting the coastal response to future hydrodynamic forcing is a challenging task due to the significant uncertainties associated with a changing and variable climate. The climate-related factors explored here are those that are likely to have a significant impact on future water levels and, therefore, the amount of coastal change that could potentially occur. These factors include sea level, wave climate, and the frequency of major El Niños. Various combinations of projected trends for these three factors are considered to evaluate the role of a changing climate on coastal vulnerability. The present (2009) and years 2030, 2050, and 2100 are chosen to examine the evolution of coastal change hazards and community exposure through time to both the annual and 100-year event.

3.2.1 Sea-level Rise

Over the 20th century, global mean sea level rose ~20 cm with an average rate of about 1.7-1.8 mm/yr (Church and White, 2006; Jevrejeva et al., 2006; Holgate, 2007). The rate of sea-level rise (SLR) has accelerated over the last few decades, reaching rates of 2.8-3.4 mm/yr as measured by satellite altimetry (Leuliette et al., 2004; Cazenave and Nerem, 2004; Bindoff et al., 2007; Nerem et al, 2010). Rising sea levels can have

potentially devastating effects on coastal communities as the risk of inundation and shoreline retreat increases.

According to the Intergovernmental Panel on Climate Change (IPCC), increases in sea level are consistent with trends in global warming (Bindoff, 2007). Furthermore, the recent increase in global temperature is "very likely" attributed to an increase in anthropogenic greenhouse gas concentrations (Hegerl, 2007). Therefore, the amount that global mean temperature, and thus sea level, will rise in the future is largely dependent on overall global carbon emissions. In 2000, the IPCC Special Report on Emissions Scenarios (SRES) defined a series of scenarios to describe possible alternative world states over a range of future emissions (Nakicenovic et al., 2000). These SRES emissions scenarios are the basis of most SLR projections due to the global recognition and acceptance of the IPCC reports.

Due to uncertainties associated with the underlying physical processes that drive SLR, projections for the magnitude and rate of SLR in the future can vary substantially depending on the models and methods applied. The most recent IPCC Assessment Report (AR4), suggested that global sea level may rise 0.18 to 0.59 m above the 1990 level by the year 2100 (Meehl et al., 2007). These projections, made using physics-based climate models, do not reasonably address the dynamical responses of ice sheets, however, and IPCC authors have suggested that an additional 0.1-0.2 m of rise by the end of the century is likely. Pfeffer et al. (2008) made an attempt to constrain SLR estimates that include ice flow dynamics, concluding that projections of 0.8-2.0 m by 2100 are physically possible.

Recently, an alternative approach for estimating future sea levels, without having to model complex glacial processes, has been developed. Semi-empirical techniques, first published by Rahmstorf (2007), allow for climate researchers to indirectly estimate SLR in response to changes in global mean surface temperatures based on statistical relationships. Unlike the current physical models, observationally-tuned semi-empirical models are able to successfully reproduce historic trends in SLR (Rahmstorf, 2007; 2010). These statistical models have resulted in estimates of 0.5-1.4 m (Rahmstorf, 2007), 0.5-1.0 m (Horton et al., 2008), 0.9-1.3 m (Grinsted et al., 2009), 0.75-1.90 m (Vermeer and Rahmstorf, 2009), and 0.6-1.6 m (Jevrejeva et al., 2010) of SLR by 2100 for the full range of SRES scenarios.

Because future SLR estimates vary depending on the details of the methods used and are constantly being refined as new data becomes available, a range of future projections is used here for the development of the climate change scenarios rather than using the results of any one particular model or research group. For consistency, so as to not introduce too many variables, SLR values from the most current semi-empirical estimates for the A1B SRES emissions scenario only are compiled. The A1B scenario describes a more integrated world characterized by rapid economic growth, technological innovation, increased globalization, and a balance across energy sources so that we are not solely reliant on fossil fuels (Nakicenovic et al., 2000).

Using curves published by Horton et al. (2008), Vermeer and Rahmstorf (2009), Grinsted et al. (2009), and Jevrejeva et al. (2010), SLR estimates for 2030, 2040, 2050, 2070, 2080, and 2100 were extracted. Most authors begin their projected SLR curves

from the 1990s to be comparable with IPCC projections. The values were adjusted to be relative to 2010 for ease of integration with the other data used to create the climate change scenarios. To do this, an estimate of the current global SLR rate as measured via satellite altimetry from the University of Colorado Sea Level Change group for 1992-2010 of 3.2 ± 0.4 mm/yr (http://sealevel.colorado.edu/index.php, retrieved 18-Aug-10) was used. Per this rate, a SLR of 6.4 cm over the last two decades was subtracted from the raw semi-empirical estimates. A quadratic was fit through the average of all the middle or "best guess" curves published by the authors to create a medium SLR projection. In some cases, a range around the A1B scenario was available (e.g., Grinsted et al., 2009; Jevrejeva et al., 2010). Another quadratic curve was fit through the maximum of the estimates for the high end of this range. Similarly, a third curve was fit through the minimum of the low estimates, producing the high and low SLR projections, respectively (Figure 2). These curves yield synthesized estimates of future sea level for the time periods of interest – 2030, 2050, and 2100.

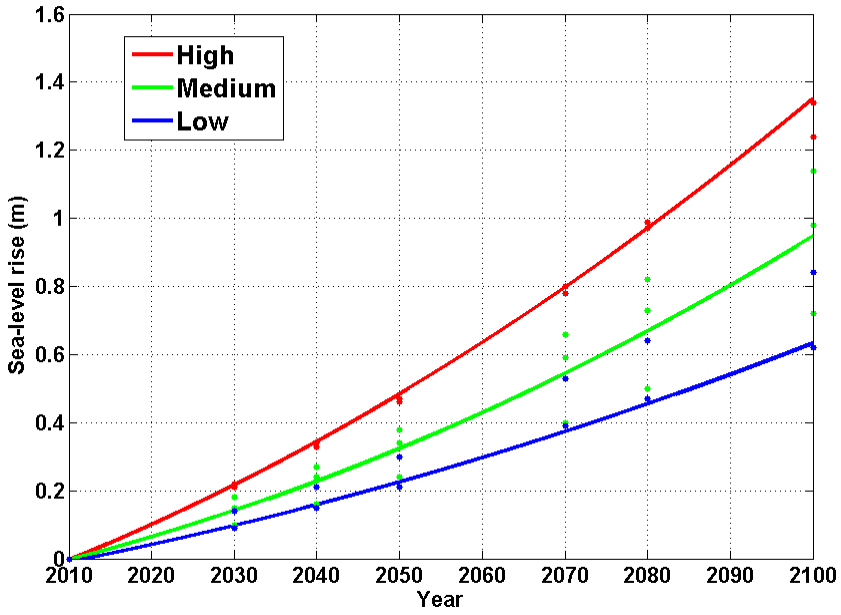

Figure 2. Global sea-level rise projections through 2100. High (red), medium (green), and low (blue) curves were fit through recent semi-empirical estimates for the A1B emissions scenario (shown as dots, color coded for their respective curve).

Sea-level rise, however, is not spatially uniform over the entire globe, as can be seen from tide gauge measurements and sea surface height maps derived from altimetry data. This regional variability can be attributed to nonuniform warming and cooling of the ocean, freshwater exchange with the atmosphere and land, and redistribution of ocean mass through advection and diffusion (Wunsch et al., 2007). For example, there was a ~10-15 mm/yr difference in the rate of SLR between the eastern and western Pacific between 1993-2008; rates in the western equatorial region were up to three times faster than the global mean but rates along the West Coast of the U.S. were lower (Cazenave and Llovel, 2010). In the PNW, local rates of SLR are also influenced by alongshore varying rates of vertical land movement, or uplift, along the coast related to the Cascadia Subduction Zone where the underlying oceanic and continental plates are colliding. The

southern Oregon coast is uplifting faster than the present regional rate of SLR and is therefore emergent, while the central coast is rising at a slightly lower rate and is experiencing a relative rise in sea level (Komar, 1998, Komar et al., in press). The global SLR estimates from the curves in Figure 2 were modified to reflect local tectonics for application to the study area (Table 1) where the average rate of uplift is approximately 1 mm/yr (Burgette et al., 2009; Mazzotti et al., 2008). While uncertain, this rate is assumed to be constant through the end of the century, resulting in 0.09 m of uplift between 2010 and 2100.

Table 1. Relative sea-level rise (SLR) values, in meters, for the north-central Oregon coast for low, medium, and high scenarios as interpolated from the curves in Figure 2 and adjusted for 1 mm/yr of uplift at the time periods of interest, relative to 2010.

SLR Scenario	2030	2050	2100
Low	0.08	0.18	0.54
Medium	0.12	0.28	0.86
High	0.20	0.45	1.26

3.2.2 Wave Climate

In addition to threats of rising sea levels over the next century, the Oregon coast is also at risk to extreme waves generated by large winter storms. During these events, elevated water levels, caused by a combination of wind, wave, and barometric effects, increase the likelihood of wave runup reaching coastal dunes, resulting in erosion. While the wave climatology of the PNW is already recognized for its power and severity, increases in storm intensities and wave heights over the period of historical measurement

have been documented by several researchers (e.g., Allan and Komar, 2000; 2006; Méndez et al., 2006; Ruggiero et al., 2010).

According to rates published by Ruggiero et al. (2010), annual average significant wave heights have increased by almost 50 cm since the mid-1970s, or 1.5 cm/yr. This trend, however, is dampened by waves occurring during the summer months when wave heights are typically lower. In the winter, when most of the large storms occur in the PNW, monthly mean wave heights have been increasing at a slightly faster rate of 2.3 cm/yr. Averages of the five largest significant wave heights recorded each year exhibit a rate of increase of 7.1 cm/yr, while even larger still is the rate of increase for the annual maximum wave heights of almost 10 cm/yr indicating that the most extreme waves that occur each year have increased by over 3 m, from 9 m in the late 1970s to over 12 m presently. Simply put, larger waves are getting bigger faster. This observation has significant implications for coastal areas which are growing increasingly vulnerable to the large waves.

While some researchers have attempted to make a link between warmer ocean temperatures in the western Pacific and increasing storm intensities off the PNW coast (e.g., Graham and Diaz, 2001), attributing this increase to human-induced climate change is not yet definitive because the wave height record only goes back a few decades, complicating our ability to make projections of future conditions. For this reason, a set of simple wave height scenarios was developed for use in conjunction with the projections of sea-level rise that attempt to incorporate future uncertainty by covering a range of possibilities. Assessments of coastal vulnerability that do not account for potential

changes in wave climates may be of limited value as Ruggiero (2008) demonstrated that increasing wave heights can be as important or more important than relative SLR in terms decadal scale changes in TWLs.

High, medium, and low scenarios for wave height trends through 2100 were developed to represent conditions where significant wave heights continue to increase at their present rate until 2030 and remain high through the end of the century, stay at their present levels indefinitely, or decrease until 2030 (at the same rate at which they have been increasing) and remain low (Figure 3). Projections for rates of change were truncated after 20 years (2030) due to the significant uncertainty associated with how the wave climate will evolve as time progresses. Because wave heights of different magnitudes are currently increasing at different rates, as demonstrated by Ruggiero et al. (2010), wave heights were allowed to change depending on their exceedance percentile of the wave height cumulative distribution function. The average rates of increase (decrease) prescribed to waves within each of four quartiles for the high (low) wave height scenarios are 1 cm/yr, 1.5 cm/yr, 2 cm/yr, and 4 cm/yr.

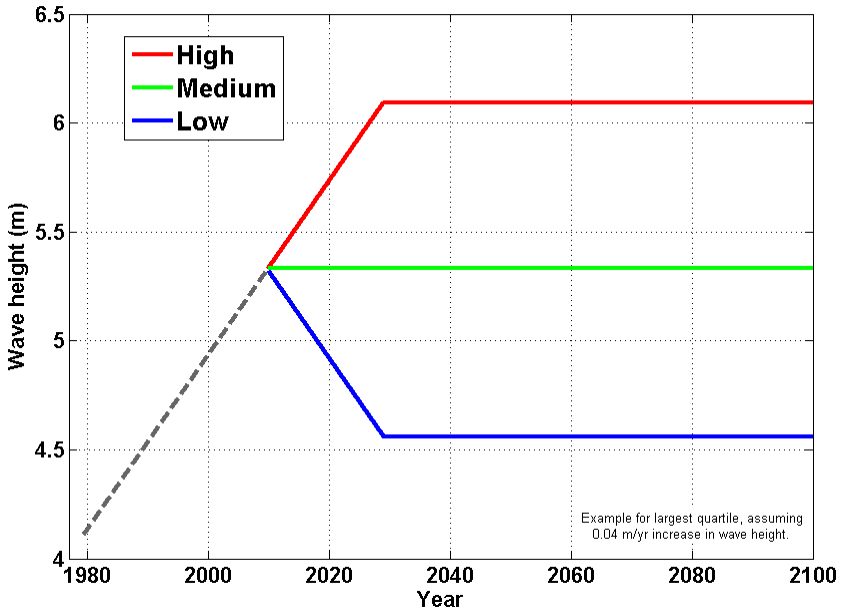

Figure 3. Example projections for wave heights through 2100. High (red), medium (green), and low (blue) scenarios are shown for the largest quartile, historically exhibiting a 4 cm increase in wave heights per year (dashed gray).

3.2.3 El Niño Frequency

During El Niños, the U.S. West Coast experiences periods of elevated water levels and enhanced storm wave heights (Allan and Komar, 2006), effectively increasing the probability that wave runup will reach coastal foredunes and cause erosion. In addition, because waves during major El Niños are anomalously approaching from the southwest, significant retreat typically occurs at the southern ends of littoral cells and directly north of jetties and tidal inlets (Kaminsky et al., 1998). El Niños occur periodically as part of the Earth's climate cycle, with a major El Niño occurring about every fifteen years since the mid-1970s (Figure 4). The most notable El Niños in the recent past were those that occurred during the winters of 1982-83 and 1997-98 when monthly mean winter water levels were 20-40 cm greater than the long-term averages,

resulting in tens of meters of shoreline retreat (Kaminsky et al., 1998; Allan and Komar, 2006).

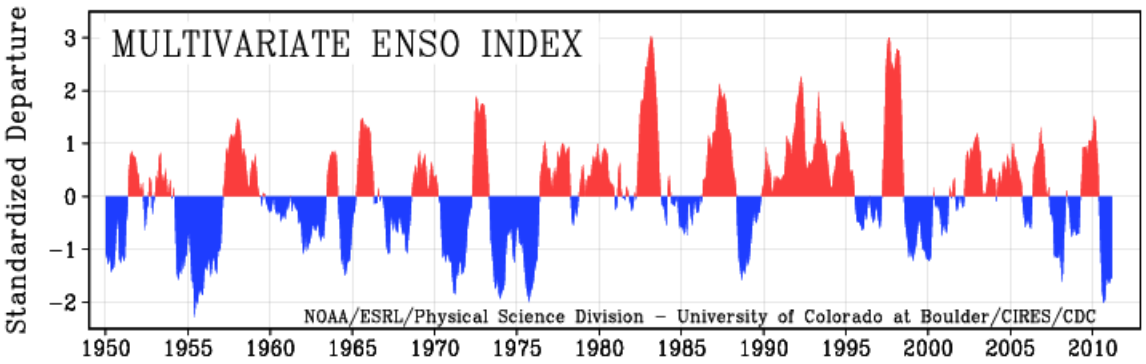

Figure 4. Historical record of El Niño occurrences (red) dating back to 1950 as measured using the Multivariate ENSO Index (MEI). Published online by K. Wolter at: http://www.esrl.noaa.gov/psd/people/klaus.wolter/MEI/.

There is no doubt that the periodic occurrence of major El Niños in the future will exacerbate the impacts of increasing sea levels and storminess, but there is much uncertainty in how the magnitude and frequency of El Niño events will evolve in a changing climate. There have been some suggestions of a recent shift towards more El Niño-like conditions based on the number of unusually high events that occurred in the 1980s and 1990s, potentially attributable to the increase in greenhouse gas concentrations also seen at this time (Trenberth and Hoar, 1997). However, it can be difficult to decipher trends from natural variability in the record as shown by Rajagopalan et al. (1997), who conclude the anomalies seen in the 1990s are not as unusual or unlikely as previously suggested. Responses of global climate models to an increase in greenhouse gases are highly variable, with some results indicating a shift towards more El Niño-like

conditions, in others less, and still others show there is no change from the present-day variability (van Oldenborgh et al., 2005; Collins et al., 2005).

For the development of the climate change scenarios, two trajectories of the frequency of major El Niño events in the future are considered. In one case, designated the "medium" scenario, the current trend of one major El Niño per fifteen years is sustained through the end of the century. In the second case, or "high" scenario, the frequency is allowed to double so that there are two major El Niños every fifteen years similar in scale to the event during the winter of 1997-98.

By combining the projections for future sea level, wave climate, and El Niño frequency as described above, a matrix of 18 possible climate change scenarios was created (Figure 5). Individual scenarios are referred to by a series of three letters that describe, in order, the particular projection of SLR, wave heights, and El Niño frequency involved, indicated by an L (low), M (medium), or H (high). These scenarios serve as the basis for how total water levels might evolve over the coming century so that the impact of various climate change components on coastal change hazards and, therefore, the vulnerability of coastal communities in the future can be evaluated.

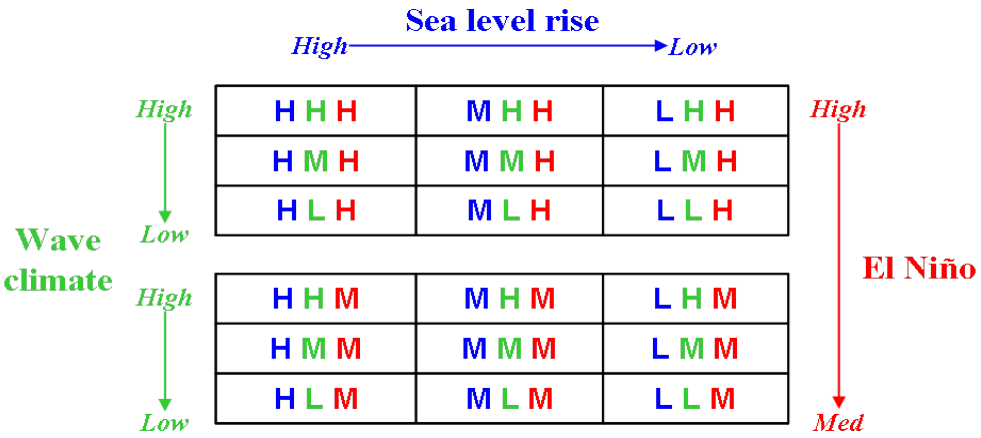

Figure 5. Matrix of 18 climate change scenarios listing the combinations of low, medium, or high projections for sea-level rise, wave climate, and the frequency of major El Niño events considered.

3.3 Erosion Models

Because the focus of this thesis is on developing an approach to assess coastal change hazards and vulnerability, relatively simple models that typically result in conservative estimates of erosion are applied here. The second term in Equation 1, $CC_{climate}$, is addressed by quantifying the amount of landward retreat that may result from SLR using a "Bruun Rule" type calculation (Bruun, 1962; 1988). In the absence of significant sediment sources and sinks, the Bruun Rule states that the equilibrium profile of the beach and nearshore moves upward and landward in response to a rise in the mean sea level. This one-dimensional model assumes that the material eroded as the profile retreats landward is deposited immediately offshore via the principle of mass conservation, maintaining a constant water depth offshore of the "closure depth". Given a rise in sea level, S, the amount of landward retreat, $CC_{climate}$, is found using

$$CC_{climate} = \frac{L}{B+h} S \qquad (2)$$

where L is the cross-shore distance to the water depth, h, the depth beyond which significant gradients in sediment transport do not occur (the closure depth), and B is the elevation of an onshore feature (such as a berm) or contour. The term $L/(B+h)$ is equivalent to the shoreface slope, $\tan \beta_{sf}$, so the Bruun Rule can be rewritten as

$$CC_{climate} = \frac{S}{\tan \beta_{sf}} \tag{3}$$

As sea level rises, the shoreface slope is assumed to remain constant while the dune toe elevation becomes higher relative to the land. This change is accounted for during the calculation of CC_{event}, as described further below.

In addition to long-term coastal retreat due to SLR, the coastal change hazard zones accommodate erosion that takes place during large storm events or periods of elevated water levels, such as during El Niños, in the form of wave-induced erosion of the foredune. The amount of erosion that occurs depends on the elevation of the TWL relative to the toe of the foredune (Ruggiero et al., 1996; 2001). In its most general form, the TWL is defined as

$$\text{TWL} = \overline{\eta} + \eta_a + \eta_r + R \tag{4}$$

where $\overline{\eta}$, the time-average water level or mean sea level, η_a, the astronomical tide level, and η_r, the non-tidal residual water level (i.e., storm surge and other oceanographic factors that raise or lower water levels), make up the measured tidal elevation, E_T, and R is the wave runup, composed of both setup and swash, here calculated using the 2% exceedance value of swash maxima as defined by an empirical relation for extreme wave

runup by Stockdon et al. (2006). When these substitutions are made, the TWL equation becomes

$$\mathrm{TWL} = E_T + 1.1\left(0.35\tan\beta_{bs}\left(H_0 L_0\right)^{1/2} + \frac{\left[H_0 L_0\left(0.563\tan\beta_{bs}{}^2 + 0.004\right)\right]^{1/2}}{2} \right) \quad (5)$$

where $\tan\beta_{bs}$ is the beach slope, H_0 is the deep-water wave height, and L_0 is the deep-water wave length, given as $\left(g/2\pi\right)T^2$ where g is the acceleration due to gravity and T is the peak wave period. This formula is applicable over a variety of beach conditions, ranging from dissipative to reflective, and thus suitable for all dune-backed beaches in the study area. Because the focus here is on extreme TWLs, in which runup can occur over the entire beach face, the backshore beach slope is used, defined as the slope between the mean high water (MHW) shoreline contour and the dune toe.

To statistically determine extreme TWLs for the annual and 100-year return level at each time period of interest, the peak-over-threshold (POT) method of extreme value theory is applied (Coles, 2001). In this method, a high threshold, u, is chosen and exceedances over this threshold are analyzed. It is assumed that the number of exceedances in a given year follows a Poisson distribution with annual mean vT, where v is the event rate and T = 1 year, and that the threshold excesses $y > 0$ are modeled using the Generalized Pareto Distribution. The N-year return level, y_N, is given as

$$y_N = u + \frac{\sigma}{\xi}\left[\left(Nn_y\zeta_u\right)^{\xi} - 1\right] \quad (6)$$

where σ is a scale parameter, ξ is a shape parameter, n_y is the number of observations per year, and ζ_u is the probability of an individual observation exceeding the threshold. Here the threshold value is set such that, on average, five TWL events per year are analyzed, a value equal to about the 97-98th exceedance percentile of the overall climatology. While this application of extreme value theory assumes stationarity in the TWL time series, climate change-induced trends in the TWL are accounted for by calculating extreme values separately for each time period of interest, as discussed later in more detail.

When the TWL exceeds the elevation of the dune toe during extreme events, waves begin to impact the dune and erosion occurs (Figure 6). To quantify the amount of coastal change that can take place during a period of elevated TWLs, the simple K99 geometric foredune erosion model is used. According to this model, the dune toe will retreat upward and landward as a function of the maximum TWL experienced during a large event, while maintaining a constant backshore beach slope. The maximum expected storm-induced dune erosion, DE_{max}, is calculated as

$$DE_{\max} = \frac{\mathrm{TWL}_{event} - E_J}{\tan \beta_{bs}} \tag{7}$$

where E_J is the elevation of the junction between the dune and the beach face, or the toe of the dune, and $\tan \beta_{bs}$ is the backshore beach slope.

The K99 dune erosion model is typically fairly conservative (Mull, 2010), primarily because the equation does not take into account the length of time in which the beach is experiencing high water levels. With no time dependency, the model likely over

predicts the amount of erosion that might actually occur during a single storm event or extreme high tide.

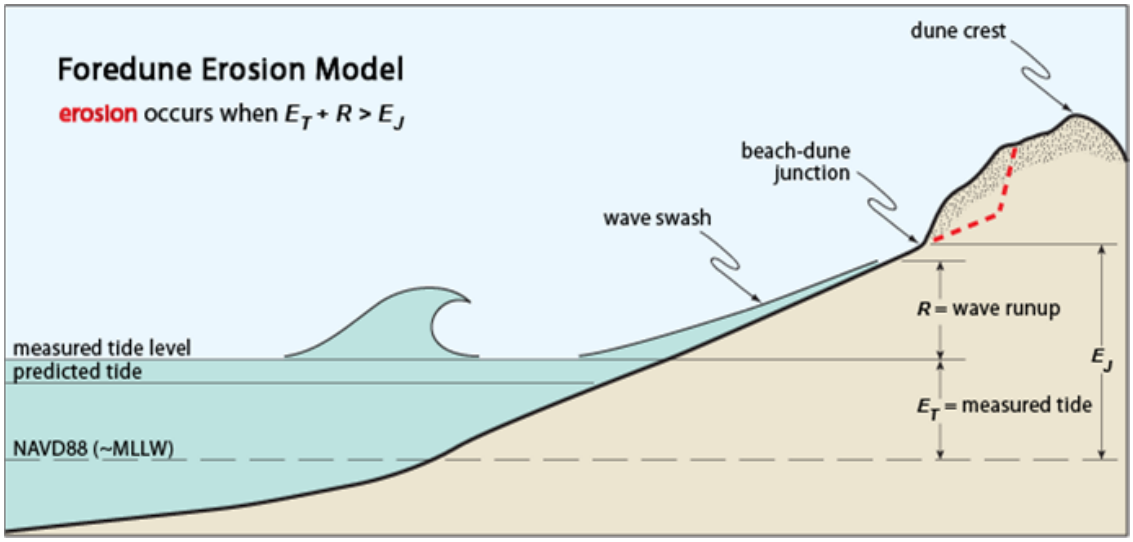

Figure 6. Total water level (TWL)-based, foredune erosion model (after Komar et al., 1999; Ruggiero et al., 2001). An extreme TWL event ($E_T + R$) that exceeds the elevation of the dune toe, E_J, will cause erosion of the foredune until equilibrium with the elevated TWL is reached.

To account for the long-term effect of SLR, which acts to move the dune toe elevation landward and upward, E_J is adjusted by the change in sea level, S, that occurs over the time period of interest so that for the application presented here, the amount of coastal change that takes place during, for example, the annual or 100-year return TWL event is

$$CC_{event} = \frac{\mathrm{TWL}_{event} - \left(E_J + S\right)}{\tan \beta_{bs}} \tag{8}$$

In the case of the increasing wave height scenarios, the approach outlined here incorporates non-stationarity into analyses of the extremes. For example, the 100-year

event in 2030 can be very different than the present-day 100-year event depending on wave height trends in the future (Ruggiero, 2010).

In order to apply this approach and quantify coastal change hazards, the morphology of the study area (e.g., tan β_{sf}, tan β_{bs}, and E_J) must first be characterized and the appropriate hydrodynamic inputs, including wave heights, periods, and tides, are determined so that future extreme TWLs can be calculated.

3.4 Morphometric Inputs

Shoreface slopes were calculated by finding the slope between the approximate multidecadal depth of closure and the mean high water (MHW) shoreline (2.1 m contour, relative to NAVD88), derived from light detection and ranging (LiDAR) data. Nearshore bathymetry was extracted at 500 m intervals from a 6 arc-second digital elevation map of the central Oregon coast obtained from the National Geophysical Data Center (NOAA Center for Tsunami Research, 2004). The 20-m isobath was chosen for estimating shoreface slopes; however, results were fairly insensitive to a range of reasonable values (15-25 m). The 500-m resolution of alongshore varying shoreface slopes was interpolated to match the more highly resolved – and variable – beach morphometrics.

The remaining morphometric parameters used in this study were derived from high-resolution LiDAR data collected in September 2002 as part of the Airborne LiDAR Assessment of Coastal Erosion (ALACE) project performed by NASA and the USGS (NOAA Coastal Services Center, 2002). Mull (2010) extracted several beach and foredune parameters for all of the dune-backed beaches in Oregon and southwest

Washington from the LiDAR dataset using automated techniques first developed by Plant et al. (2002) and Stockdon et al. (2009) for the southeast U.S. coast, which were adapted for the PNW. As a result, morphometric parameters relevant to this study, the elevation of the dune toe and the backshore beach slope, were defined for thousands of cross-shore profiles every few meters along the coast.

While highly resolved in the alongshore, this LiDAR dataset serves only as a single snapshot of beach and dune geomorphology. The coast, however, is a dynamic environment that evolves over many timescales. There are also both measurement and extraction errors associated with the derived morphometrics. Inclusion of this morphological uncertainty and variability is necessary for accurately assessing the uncertainty of future coastal hazards, as the magnitude of storm-induced coastal erosion is influenced by the beach slope and dune toe elevation at the time when an elevated TWL event occurs (refer back to Equation 8).

To account for morphometric uncertainty, foredune toe elevations were randomly sampled from a normal distribution (for N iterations) where the mean is the value extracted from the LiDAR data and the standard deviation is defined by the vertical error associated with its selection and interpolation, mean total RMSE = 0.66 m (Mull, 2010). The backshore beach slope is also allowed to vary but in a different manner. Similar to Ruggiero and List's (2009) technique for estimating historical beach slopes in the absence of long-term measurements, the highly-resolved spatial variability in the LiDAR dataset is used as a proxy for temporal variability. First, the shoreline in each littoral cell is divided into approximately 1-km segments, being mindful of tidal inlets and headlands.

From the distribution of beach slopes within each segment, the median and standard deviation were determined. Because a traditional 95% confidence interval may encompass slopes that are less than zero, especially if the 1-km segment contained several very low slopes, the uncertainty around the median beach slope is defined using the lesser difference between the 95% and 50% exceedance statistics or the 50% and 5%. This uncertainty statistic is divided in half and used as a substitute for the standard deviation of the beach slopes. Figure 7 illustrates an example beach slope distribution for a 1-km segment of the coast in the Rockaway littoral cell. The median and standard deviation are used to define a normal distribution from which beach slopes are randomly sampled (N times) for each alongshore profile. By incorporating the spatial variability within a 1-km stretch of shoreline, beach level variations due to rip current embayments (i.e., CC_{HS} from Equation 1) are indirectly accounted for.

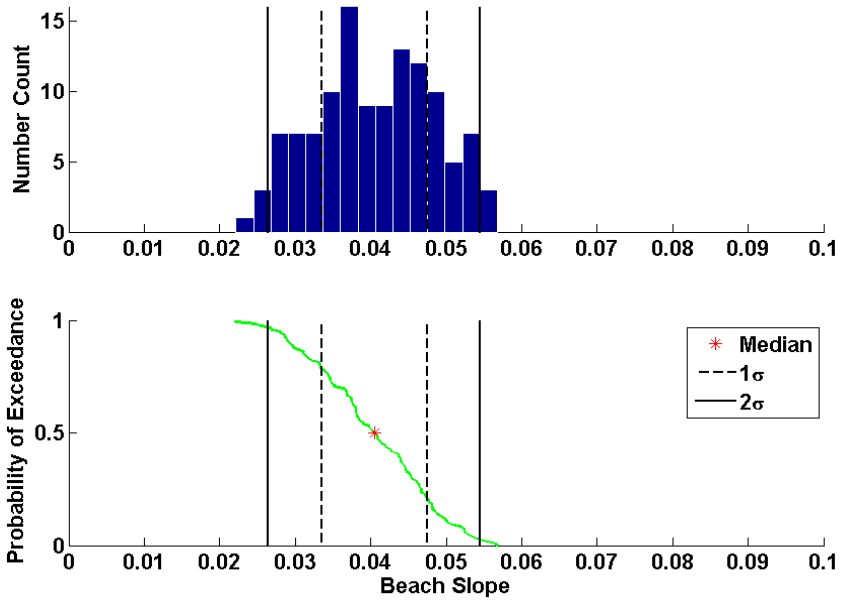

Figure 7. Example backshore beach slope distribution (top) and probability of exceedance curve (bottom), showing the median and associated confidence interval for a 1-km segment in the Rockaway littoral cell.

To optimize the number of iterations to perform when randomly sampling from the morphological parameters, the cumulative standard deviation of the alongshore-averaged mean total erosion distance for CC_{event} (using Equation 8), which is shown in Figure 8, is examined. The appropriate number of iterations, N, was defined as when significant changes in the cumulative standard deviation reached zero. Ultimately, 100 iterations of random dune toe and slope configurations for each of the 18 climate change scenarios were performed, resulting in 1800 estimates of storm-induced coastal change at each of several thousand (in the alongshore) LiDAR-derived profiles.

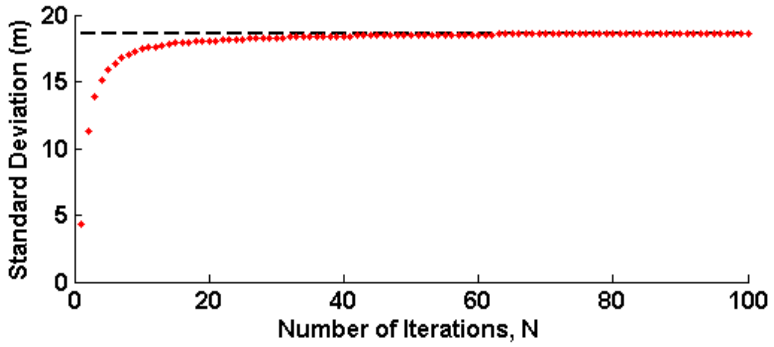

Figure 8. Cumulative standard deviation of the alongshore-averaged mean total erosion distance achieved by increasing the number of morphological configurations used.

3.5 Hydrodynamic Inputs

After characterizing the local geomorphology, the next step in the approach is to quantify the extreme total water levels (TWLs) given the suite of climate change scenarios. First, historical time series of relevant wave parameters and tidal elevations were constructed by Harris (2011), whose methods are briefly described here. After a series of transformations to normalize measured wave conditions from several deep-water buoys off the coast of northern Oregon, as complete as possible combined record of wave

heights and periods was developed. The resulting dataset was > 80% complete, extending from late 1976 through the end of 2008. Next, hourly tide data was acquired from the Yaquina Bay tide gauge, located ~50 km south of Tillamook County, as it has the longest, most continuous record of water levels for the north-central Oregon coast. The tide data was corrected to account for subsidence of the reference benchmark from 1967 to 1996 (Burgette et al., 2009).

Harris (2011) used these historical datasets to develop a set of synthetic time series through the end of the 21st century by repeatedly appending the last 30 years of data to the original time series and applying the prescribed climate change scenarios to the wave height and water level components (Figure 9). As a result, 18 sets of wave and tide time series were created that vary based on the combination of low, medium, and high projections for future wave climate, sea-level rise, and occurrences of major El Niños.

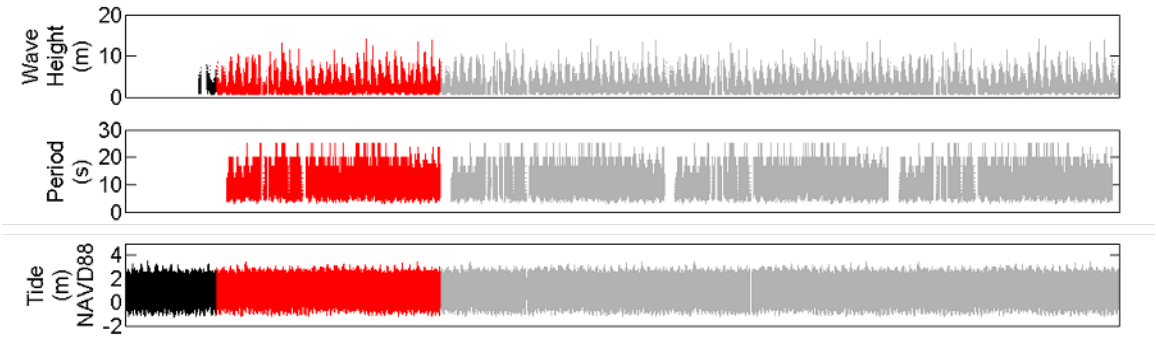

Figure 9. Example wave height, period, and tide time series from Harris (2011) showing the 30 years of data (red) used to create the synthetic datasets (gray) which extend the historical data to 2100 without any climate change trends incorporated. Data prior to 1979 (black) was not used.

Based on the synthetic wave datasets, individual time series of wave runup were calculated for 30 backshore beach slopes that cover the range of naturally occurring beach slopes on the northern Oregon coast, ranging from 0.005 to 0.15 at increments of 0.005. These runup time series were subsequently added to the hourly tide data to develop 18 TWL time series (per beach slope) extending from 1976 to 2100, one for each of the climate change scenarios (Figure 5). Using Equation 6, these synthetic TWL time series allow us to compute extreme return levels at any time over the next century. Here extreme TWL events for the annual and 100-year return level (more commonly referred to as the 100% and 1% annual chance events) are calculated for 2009, 2030, 2050, and 2100 using only the 30 years of data prior to the time period of interest in order to emphasize the non-stationarity in the synthetic datasets.

Because the extreme TWLs vary smoothly across the range of beach slopes, lookup tables of the extreme values through time are developed and can be used to interpolate extreme TWL values for any slope. For the 18 climate change scenarios and 100 combinations of slope and dune toe parameters, 1800 sets of extreme TWLs for each event at each time period of interest are calculated by interpolating from the lookup tables. The resulting extreme TWLs were used in conjunction with the derived morphometrics to quantify future coastal change hazards using Equations 3 and 8.

3.6 Assessing Community Exposure

To reduce risk, it is not only important to determine the impending physical impacts of coastal hazards but it is also necessary to explore the vulnerability of the

human-environmental system in the context of these hazards (Berkes, 2007). Communities will have varying exposure to coastal change hazards, dictated by their distribution of assets and proximity of development to the ocean. To assess the exposure of coastal communities to future coastal change hazards, the physical model-based erosion estimates were integrated with socioeconomic data using a geographic information system (GIS).

A dataset of all the structures along the Tillamook County coast, including homes, businesses, hotels, etc., was digitized via a combination of aerial photo interpretation and field-based reconnaissance. A GIS layer of all roads and highways in Tillamook County (last updated in 2008) was acquired from the county's webpage, accessed online at: http://www.co.tillamook.or.us/gov/gis/. These data layers were overlaid with the hazard zones (described in detail later) generated for each year and event of interest. Exposure analyses were conducted by performing simple queries of these data layers in ArcGIS (version 9.3.1; ESRI, Redlands, CA) to identify structures and roads at risk to future coastal change hazards within the county. The Intersect tool was used to determine the number of structures located within a given hazard zone. The roads within the hazard zones were also identified using the Intersect tool, and then the Calculate Geometry function was used to calculate the exact length of road exposed.

4. APPLICATION TO TILLAMOOK COUNTY

Here the methodology is applied to the dune-backed beaches of Tillamook County. First is a description of the local geomorphology, followed by the extreme total water levels computed for each LiDAR-derived cross-shore beach profile. Next, the magnitudes of coastal change expected to occur for each time period of interest and design event are quantified. The resulting coastal change hazard zones developed for the county are then discussed and results from the subsequent exposure analyses are presented.

4.1 Beach Morphology

The beach and foredune morphology of the Tillamook County coast varies both within and among the four littoral cells (Figure 10). The mean and standard deviation of the relevant parameters extracted from the 2002 LiDAR data are summarized in Table 2. The dune toe and dune crest elevations averaged for the entire county are around 5 m and 11 m, respectively. The dune-backed beaches in the Netarts littoral cell have the highest mean dune crest elevation (13.6 ± 4.1 m) but one of the lowest mean dune toe elevations (4.8 ± 0.6 m), suggesting that while these dunes are relatively more vulnerable to wave-induced erosion, they may not be as likely to overtop. These high dunes are accompanied by the steepest mean backshore beach slope of the Tillamook County coast (0.051; the average for the entire county is 0.039, or 1V:25H). The smallest dunes are found in the Rockaway littoral cell, where the average dune crest elevation is 8.4 ± 1.7 m, though the dune toe elevation is slightly above the county average at 5.2 ± 0.8 m.

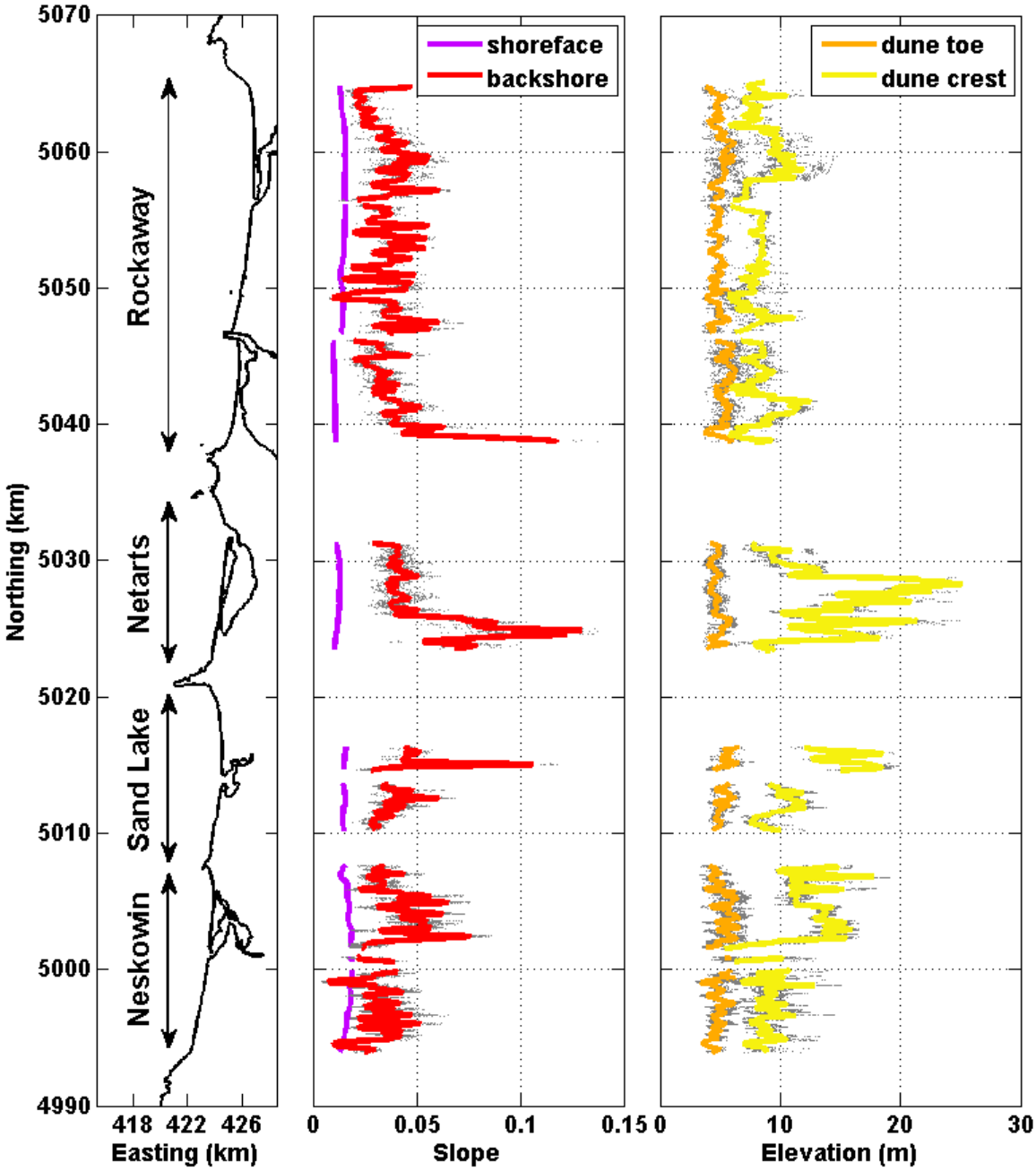

Figure 10. Alongshore varying morphometrics for dune-backed beaches in Tillamook County. The left panel shows the shoreline position for the entire county and the subdivision of the four littoral cells. The middle panel shows the shoreface (purple) and backshore beach slopes (red). The right panel shows dune toe (orange) and dune crest (yellow) elevations, in meters. For each parameter, the gray dots represent the raw data while the colored lines are the values smoothed in the alongshore direction to eliminate variability less than 250 m using a quadratic loess filter (Plant et al., 2002).

Table 2. Summary of beach and foredune parameters for the littoral cells of Tillamook County, as extracted from the 2002 LiDAR data (Mull, 2010). Elevations are relative to NAVD88, in meters.

Littoral Cell	Shoreface Slope		Backshore Slope		Dune Toe Elev. (m)		Dune Crest Elev. (m)	
	mean	std	mean	std	mean	std	mean	std
Rockaway	0.013	0.002	0.037	0.01	5.2	0.8	8.4	1.7
Netarts	0.013	0.001	0.051	0.02	4.8	0.6	13.6	4.1
Sand Lake	0.015	0.001	0.041	0.01	5.2	0.7	11.7	3.3
Neskowin	0.017	0.001	0.037	0.01	5.1	0.9	10.8	2.7
County-wide	0.015	0.003	0.039	0.01	5.1	0.8	10.7	3.2

In both the Neskowin and Sand Lake littoral cells, there is a clear division of dune height, beach slope, and, more subtly, dune toe elevation between the northern and southern ends, divided by a natural inlet. Beaches tend to be flatter with lower dune toes and crests in the southern parts of these littoral cells, while the opposite is true to the north. These characteristics can be partly attributed to the enhanced northward sediment transport that occurs in the winter during major El Niño years, when beaches in the southern parts of littoral cells experience a net loss of sediment (Kaminsky et al., 1998). This pattern is less noticeable in the Rockaway littoral cell, as it is naturally split into three sub-cells by two coastal inlets that are both stabilized by jetties.

4.2 Total Water Levels

As discussed previously, extreme TWL values for the annual and 100-year events in 2009, 2030, 2050, and 2100 were calculated for a range of backshore beach slopes for each of the 18 climate change scenarios. Figure 11 shows the resultant curves for each

time period and event for the average of the 18 scenarios. As seen in the figure, extreme TWLs vary depending on the local beach slope; TWLs reach higher elevations on steeper beaches. These TWLs are expected to increase through time, given the range of climate projections applied.

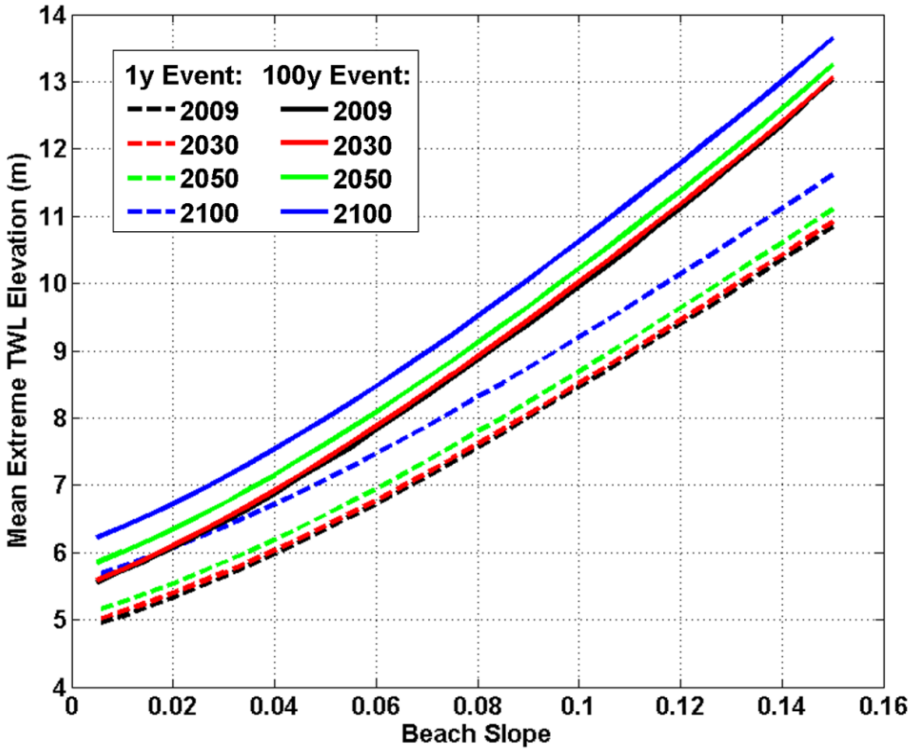

Figure 11. Extreme total water level (TWL) elevations, in meters, for a range of beach slopes. Each curve represents the mean of the 18 climate change scenarios for each time period of interest for both the annual (dashed) and 100-year (solid) return TWL event.

As the magnitude of extreme TWL events increases through time, the uncertainty in those TWLs also increases, due to the increasing uncertainty associated with each of the climate change components. This uncertainty is illustrated in Figure 12 where the range in the 18 TWL curves is plotted in relation to the mean values for each time period and extreme event of interest.

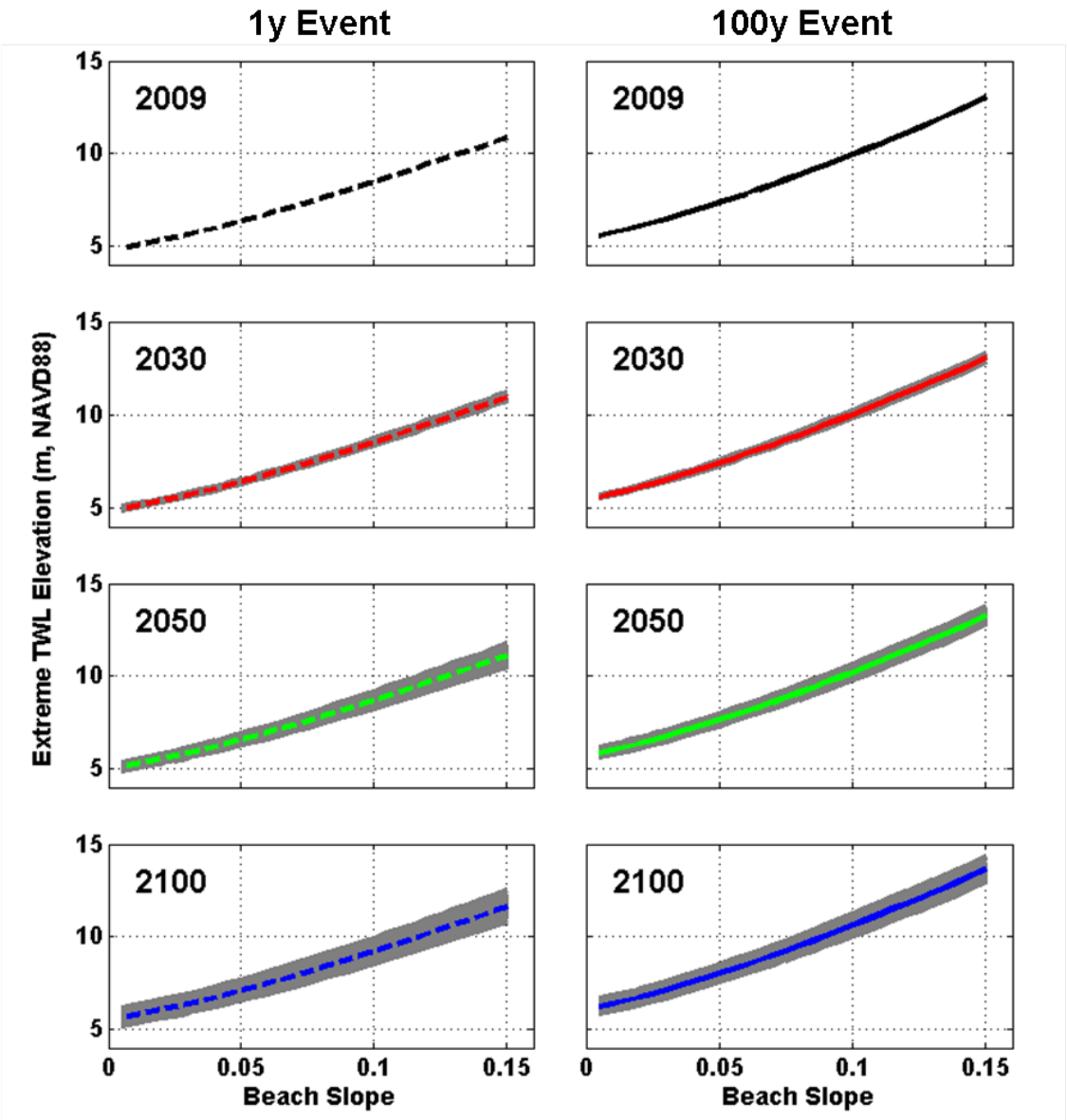

Figure 12. Uncertainty range of extreme total water level (TWL) elevations, in meters, over a range of backshore beach slopes through time, for both the 100% (left) and 1% (right) annual chance TWL events. The gray areas represent the uncertainty or range of TWLs given the 18 climate change scenarios, while the dark colored lines show the mean values which were reported in Figure 11.

At each of the cross-shore profiles in Tillamook County, for all 100 configurations of morphology, the 100% and 1% annual chance TWL elevations were interpolated from the extreme TWL curves generated for each of the 18 climate change

scenarios. Figure 13 shows the alongshore varying mean TWLs for the Neskowin littoral cell in 2009 as compared to the present-day (2002) dune toe and dune crest elevations. The mean TWL is greater than the elevation of the dune toe in almost all cases – 79% (98%) of the time for the annual event (100-year) event – indicating that some amount of storm-induced coastal change associated with these two extreme TWL events is likely under present conditions, even before any amount of SLR occurs.

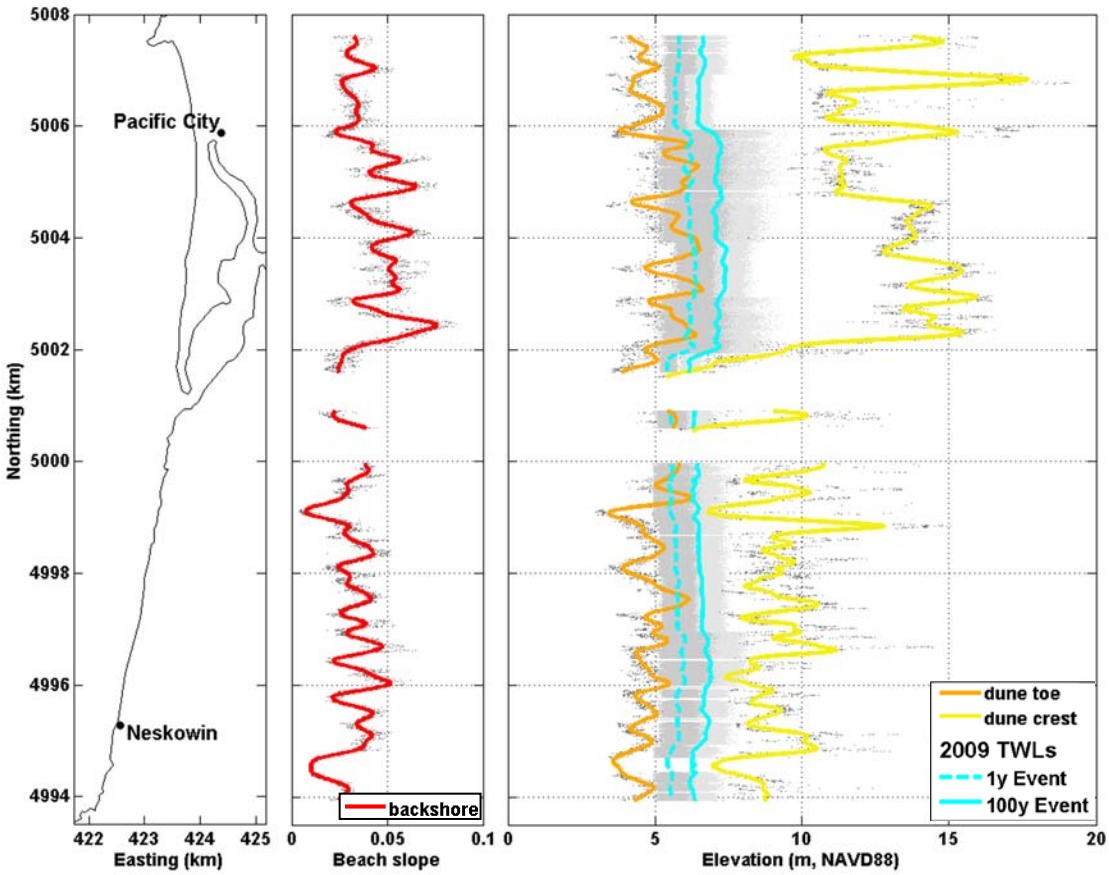

Figure 13. Example of extreme total water levels (TWLs) for the Neskowin littoral cell in 2009. The left panel shows the shoreline and location of two coastal communities in the littoral cell. The alongshore varying beach slopes (red) are shown in the middle panel. The right panel shows the mean TWLs (cyan) for the 100% (dashed) and 1% (solid) annual chance events as compared to the dune toe (orange) and dune crest (yellow) elevations. For each parameter, the gray dots represent the raw data while the colored lines are the values smoothed in the alongshore direction to eliminate variability less than 250 m using a quadratic loess filter (Plant et al., 2002).

To compare how TWLs vary through time for each of the littoral cells, the alongshore-averaged annual and 100-year return TWLs are summarized in Table 3. When averaged across all littoral cells, the 1% annual chance TWL event is found to be ~0.9 m larger than the 100% annual chance event. Throughout the century, the highest TWLs are experienced in the Netarts littoral cell because it contains the steepest backshore slopes. On average, the TWLs increase by ~0.7 m from 2009 to 2100 for the both the 100% and 1% annual chance TWL events, corresponding to a 10-12% increase.

Table 3. Overall means and standard deviations for the 100% and 1% annual chance TWL events, in meters, for each littoral cell through time (n = 1800 x the number of cross-shore profiles for each littoral cell).

Littoral Cell	Year	Annual Chance TWL Event (m)			
		100%		1%	
		mean	std	mean	std
Neskowin	2009	5.9	0.27	6.8	0.34
	2030	5.9	0.28	6.8	0.35
	2050	6.1	0.32	7.0	0.38
	2100	6.6	0.40	7.4	0.44
Sand Lake	2009	6.0	0.19	6.8	0.23
	2030	6.0	0.20	6.9	0.25
	2050	6.2	0.26	7.1	0.30
	2100	6.7	0.35	7.5	0.37
Netarts	2009	6.4	0.26	7.3	0.33
	2030	6.4	0.27	7.4	0.35
	2050	6.6	0.33	7.6	0.39
	2100	7.1	0.41	8.0	0.44
Rockaway	2009	5.9	0.21	6.7	0.26
	2030	5.9	0.22	6.8	0.27
	2050	6.1	0.26	7.0	0.32
	2100	6.6	0.36	7.4	0.38

4.3 Magnitude of Coastal Change

The total magnitude of potential coastal change estimated for each cross-shore profile results from a combination of the projected shoreline retreat associated with rising sea levels ($CC_{climate}$) and the maximum expected wave-induced foredune erosion in response to a given extreme TWL event (CC_{event}), as expressed in Equation 1. We first examine how these two components combine to produce the total predicted erosion by quantifying them individually. The results presented here do not account for existing shore protection structures (e.g., riprap), so this application demonstrates what the consequences may be if these structures are not maintained.

Figure 14 illustrates the erosion distances associated with the three SLR scenarios, the alongshore varying mean of the 1800 estimates for the 1% annual chance TWL event, and the mean total estimate of potential erosion for the Neskowin littoral cell in 2050. For this time period, the expected mean dune erosion caused by the extreme TWL event is greater than the shoreline retreat associated with both the low and medium SLR. When these variables are summarized in both the cross-shore and alongshore to compute an overall mean and standard deviation associated with each erosion component, the overall mean for $CC_{climate}$ is shown to be only half that for CC_{event} (17.9 m vs. 36.3 m; Table 4). The alongshore variability in the total mean erosion is influenced most by the variability in CC_{event}, which exhibits much greater alongshore variability than $CC_{climate}$, as a direct result of the variability in the morphological parameters from which each of the terms are calculated (tan β_{bs} and E_J vs. tan β_{sf}).

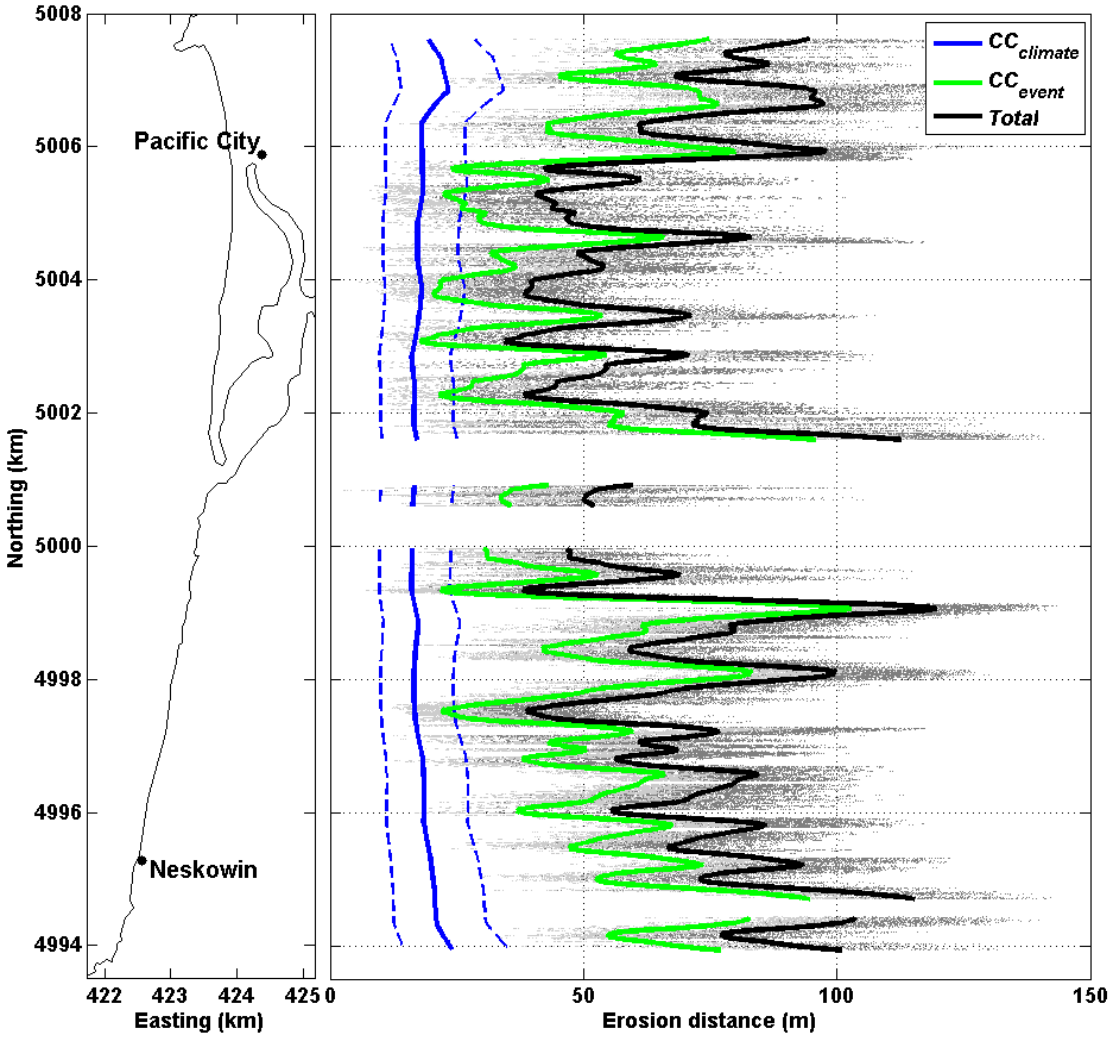

Figure 14. Example of alongshore varying mean erosion distances associated with the 1% annual chance TWL event in 2050 for the Neskowin littoral cell, in meters. The left panel shows the shoreline and location of coastal communities in the littoral cell. The panel on the right shows the potential erosion associated with the low, medium, and high SLR scenarios for $CC_{climate}$ (blue; from left to right), CC_{event} (green), as well as the total predicted mean erosion (black). For the last two parameters, the gray dots represent the raw data while the colored lines are the values smoothed in the alongshore direction to eliminate variability less than 250 m using a quadratic loess filter (Plant et al., 2002).

Table 4 summarizes the overall means and standard deviations (combining the 1800 estimates in the cross-shore with the variability in the profiles alongshore) of the total predicted erosion distances, separated into components, for comparison between the

four littoral cells. The Netarts littoral cell has the largest predicted magnitudes of erosion, ranging from 53.3 ± 19.1 m in 2009 to 124.7 ± 30.3 m in 2100 for the 1% annual chance TWL event. Though it varies slightly between littoral cells, the difference in magnitude of total erosion predicted between the 100% and 1% annual chance TWL events for any time period of interest is ~17 m. The Neskowin littoral cell is predicted to have the least amount of shoreline retreat due to increasing sea levels, as it has the steepest shoreface slopes of the county. However, because there are many areas of relatively flat beaches backed by foredunes with low dune toes, it is estimated to withstand the greatest amount of event-based coastal change throughout the century. The Rockaway and Netarts littoral cells are expected to experience the most dune retreat as the century progresses, with ~10 m (20 m) more total erosion predicted than the Neskowin and Sand Lake littoral cells for the annual (100-year) TWL event by 2100.

In 2009, 100% of the CCHZ is attributed to storm-induced erosion of the foredune associated with a given extreme TWL event. When averaged across the four littoral cells, CC_{event} is responsible for about 33 m (50 m) of erosion associated with the 100% (1%) annual chance TWL event in 2009. As the century progresses, this magnitude stays relatively constant, increasing by only 0.5-1 m. Shoreline retreat associated with rising sea levels ($CC_{climate}$), however, starts off at 0 m in 2009 and increases to ~50-70 m in 2100, depending on the littoral cell. As the magnitude of $CC_{climate}$ increases, so does its relative percentage to the total erosion until shoreline retreat due to rising sea levels becomes the dominant factor late in the 21st century (Figure 15). This shift occurs around 2070 for the annual return TWL event but not until 2090 for the 100-year event.

Table 4. Overall means and standard deviations of the predicted erosion for each littoral cell through 2100 (n = 1800 x the number of cross-shore profiles in each littoral cell).

Littoral Cell	Year	$CC_{climate}$ (m)		CC_{event} (m)				Total Erosion Distance (m)			
				100% annual chance TWL event		1% annual chance TWL event		100% annual chance TWL event		1% annual chance TWL event	
		mean	std	mean	std	mean	std	mean	std	mean	std
Neskowin	2009	0	0	35.6	23.9	51.6	28.5	35.6	23.9	51.6	28.5
	2030	7.8	3.1	35.9	24.0	51.6	28.5	43.7	24.3	59.4	28.8
	2050	17.9	6.6	36.3	24.2	52.0	28.7	54.4	25.3	70.0	29.8
	2100	51.9	17.9	36.5	24.3	52.2	28.7	88.9	30.8	104.3	34.7
Sand Lake	2009	0	0	28.6	18.2	45.1	22.6	28.6	18.2	45.1	22.6
	2030	8.7	3.4	28.7	18.2	45.1	22.7	37.5	18.5	53.9	22.9
	2050	20.2	7.2	29.2	18.5	45.4	22.9	49.4	19.9	65.6	24.2
	2100	58.6	19.5	29.4	18.6	45.5	22.9	88.1	27.1	104.2	30.4
Netarts	2009	0	0	34.1	17.0	53.3	19.1	34.1	17.0	53.3	19.1
	2030	10.6	4.1	34.2	17.1	53.3	19.2	44.8	17.5	63.9	19.5
	2050	24.4	8.8	34.7	17.4	53.5	19.4	59.2	19.3	78.0	21.1
	2100	70.9	23.9	35.0	17.5	53.8	19.4	105.9	29.3	124.7	30.3
Rockaway	2009	0	0	32.8	21.8	48.7	26.5	32.8	21.8	48.7	26.5
	2030	10.2	4.4	33.0	22.0	48.6	26.5	43.0	22.1	58.7	26.4
	2050	23.6	9.5	33.5	22.2	49.1	26.7	56.5	23.5	72.5	27.5
	2100	68.5	26.1	33.6	22.3	49.2	26.8	100.4	32.5	117.1	35.3

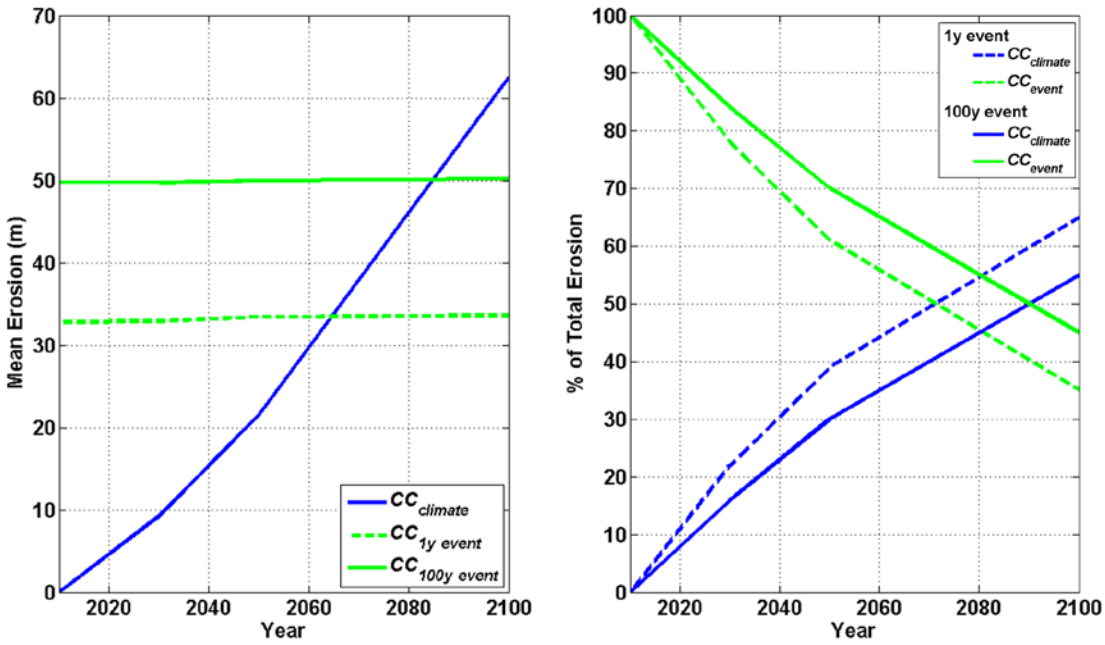

Figure 15. County-wide average of mean dune erosion, in meters, resulting from increasing sea levels ($CC_{climate}$; blue) vs. the 100% ($CC_{1y\ event}$; green dashed) and 1% ($CC_{100y\ event}$; green solid) annual chance total water level events through 2100 (left) as well as the relative percent of total erosion of each coastal change component (right).

4.4 Coastal Change Hazard Zones

At each time period of interest and for both of the extreme TWL events that have been chosen, 1800 estimates for the total magnitude of erosion were calculated. As previously mentioned, erosion associated with the 100% and 1% annual chance TWL events for 2009, 2030, 2050, and 2100 presented here serve only as an example of the extreme events and time periods that can be analyzed, and coastal managers are encouraged to choose the planning horizon and extremity of the event of interest to their community. Regardless of the event chosen, the cross-shore distribution of the resulting erosion estimates is highly alongshore variable based on the local beach geomorphology. After examining hundreds of these distributions, a Gaussian distribution was

characteristic of most of them. By assuming a Gaussian distribution of the erosion estimates, the results can be statistically summarized with the philosophy that decision-makers have the option of choosing the level of risk they are willing to accept or what confidence level should trigger a particular policy option. Here the 95% confidence interval for the magnitude of erosion expected by a certain time period is defined as the mean and ± 2 standard deviations around the mean. Figure 16 shows an example distribution of erosion estimates associated with the 1% annual chance TWL event in 2050 from the Neskowin littoral cell, highlighting the mean and 95% confidence interval chosen for one cross-shore profile.

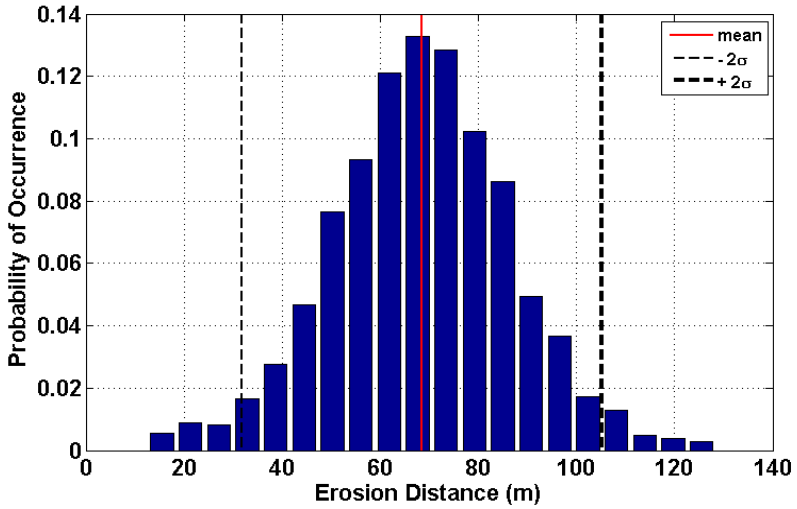

Figure 16. Example probability distribution of predicted erosion distances in the cross-shore, showing the mean (red line) and 95% confidence interval (black dashed lines); n = 1800.

The raw erosion estimates predicted from the physical models are highly variable in the alongshore due to the high-resolution of the LiDAR dataset from which the calculations are based (i.e., erosion distances are computed for thousands of profiles in each littoral cell). Presenting the data in this way would exhibit too much variation for

coastal planning purposes; therefore, the alongshore varying erosion lines are smoothed with a quadratic loess filter to eliminate variability less than 250 m (e.g., eliminating the impacts of cusps on the hazard zones; Plant et al., 2002). The mean and 95% confidence interval of the 1800 erosion estimates for all time periods of interest and both extreme TWL events for the Neskowin littoral cell, as an example, are shown in Figure 17.

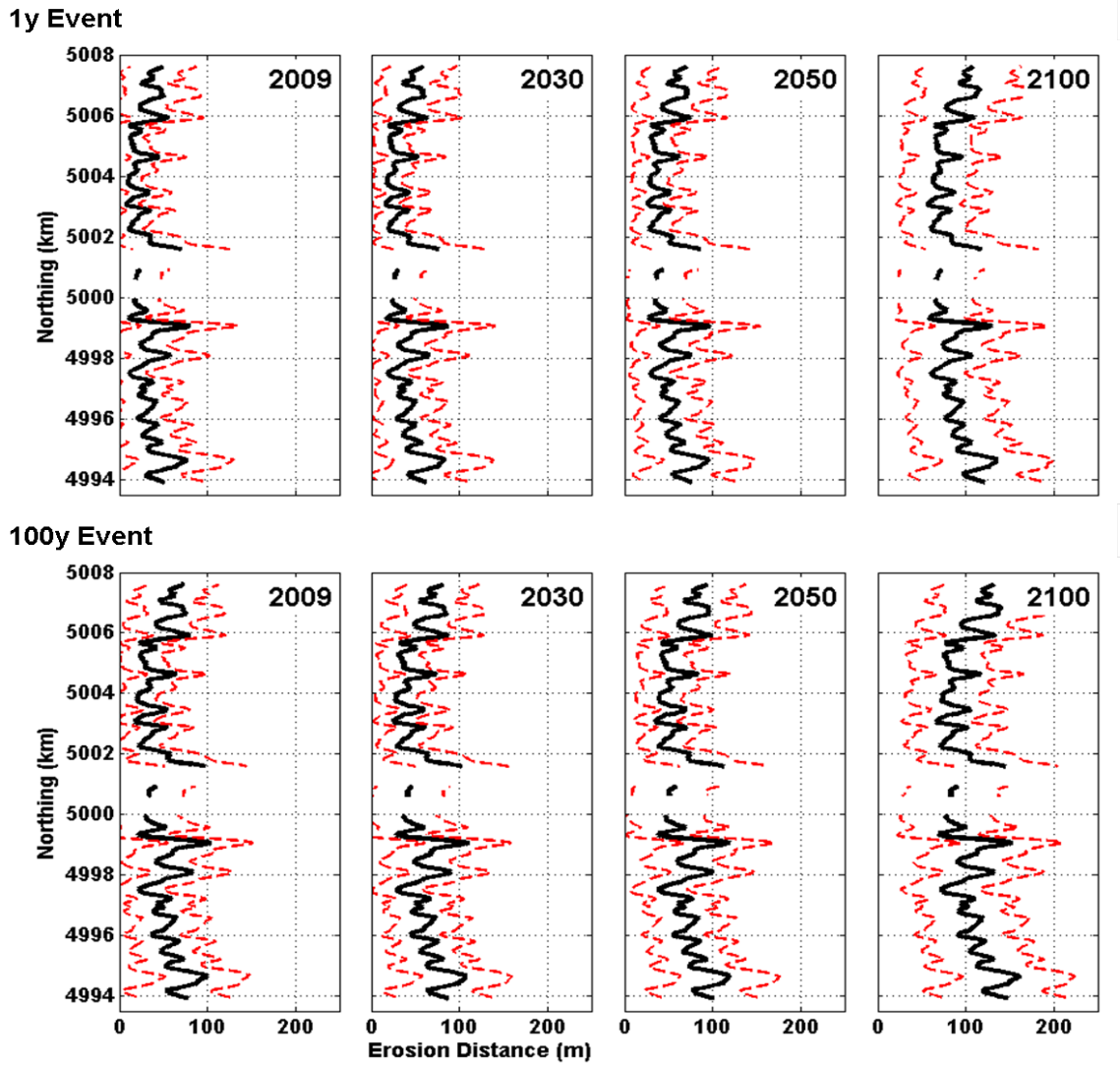

Figure 17. Total erosion distances, in meters, through time for both the 100% (top) and 1% (bottom) annual chance TWL events. In each panel, the thick solid black line represents the alongshore varying mean of the 1800 calculations while the red dashed lines represent the 95% confidence interval.

In addition to the increase in magnitude of the total coastal change hazards throughout the century, there is also an increase in the uncertainty associated with the calculations of expected coastal change as illustrated in Figure 17 (or reported as the standard deviation in Table 4). This increase has direct implications for the estimated impacts to coastal communities and shoreline properties because the hazard zones are ultimately defined based on these statistics.

From the smoothed, alongshore varying erosion distances for the mean and 95% confidence interval (Figure 17), a suite of coastal change hazard zones were defined based on the probability of erosion exceeding a certain distance. In other words, there is a 98% probability that the actual erosion will be greater than the mean - 2σ, a 50% probability it will be greater than the mean, and only a 2% probability that magnitude of erosion will be greater than the mean + 2σ (Figure 18). The two landward most zones, therefore, compose the 95% confidence interval within which the erosion for a given year and TWL event is most likely to achieve. Here, the seaward edge of the 98% exceedance probability zone is the alongshore-smoothed position of the 2002 LiDAR-derived dune toe.

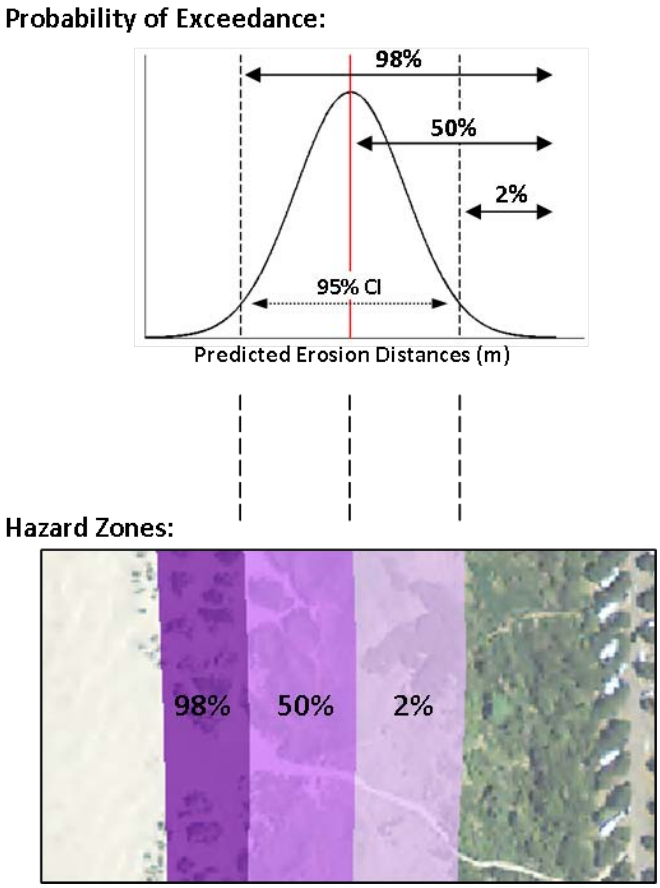

Figure 18. Conceptual diagram illustrating the delineation of the coastal change hazard zones, which are defined probabilistically based on the 95% confidence interval (CI) for the cross-shore distribution of expected erosion distances.

Coastal change hazard zones were developed for all dune-backed beaches of the four littoral cells in Tillamook County, for the annual and 100-year return TWL events in 2009, 2030, 2050, and 2100. When mapping the erosion hazards, the local geology was taken into consideration (i.e., erosion was not predicted to cut through bluffs and erosion-resistant uplands). An example of how these zones change through time for the 1% annual chance TWL event for a section of the Rockaway coast is given in Figure 19. Both the magnitude of predicted erosion and the width of the hazard zones increase through time as the erosion hazards become more severe and the uncertainty increases.

Figure 19. Coastal change hazard zones associated with the 1% annual chance TWL event for a section of the Rockaway littoral cell for 2009, 2030, 2050, and 2100.

4.5 Community Exposure to Coastal Change Hazards

The number of structures potentially at risk to coastal change hazards increases throughout the century (Figure 20). The fewest impacts to structures will be in the Netarts littoral cell because there is no coastal development along Netarts Spit, except for Cape Lookout State Park whose campground facilities have a chance of being impacted by the current 1% annual chance TWL event but are more likely to experience significant erosion problems by the year 2030.

The Rockaway littoral cell is the largest and most highly populated stretch of the Tillamook County coast, with urban development located within tens of meters of the primary foredune. In 2009, up to 281 (534) structures may be impacted by coastal change associated with the 100% (1%) annual chance TWL event. As is the case for the other littoral cells, the majority of these structures are single-family homes, condos, or apartments (258 and 488, for the 100% and 1% events, respectively). In addition to these residences, there are five overnight accommodations and 1 restaurant within the hazard zones. By the year 2050, the number of potential exposed structures increases to 536 (793) due to the 100% (1%) annual chance TWL event and then to 968 (1116) structures by 2100. This would include up to 20 overnight accommodations, a church, a bank, the police station, and 40 retail shops, offices, and restaurants.

The Neskowin littoral cell has half the number of structures within the hazard zones, though the two communities found along this region are much smaller and may sustain more significant losses as a whole. The number of exposed structures increases from 161 (253) in 2009 to 421 (507) for the annual (100-year) TWL events.

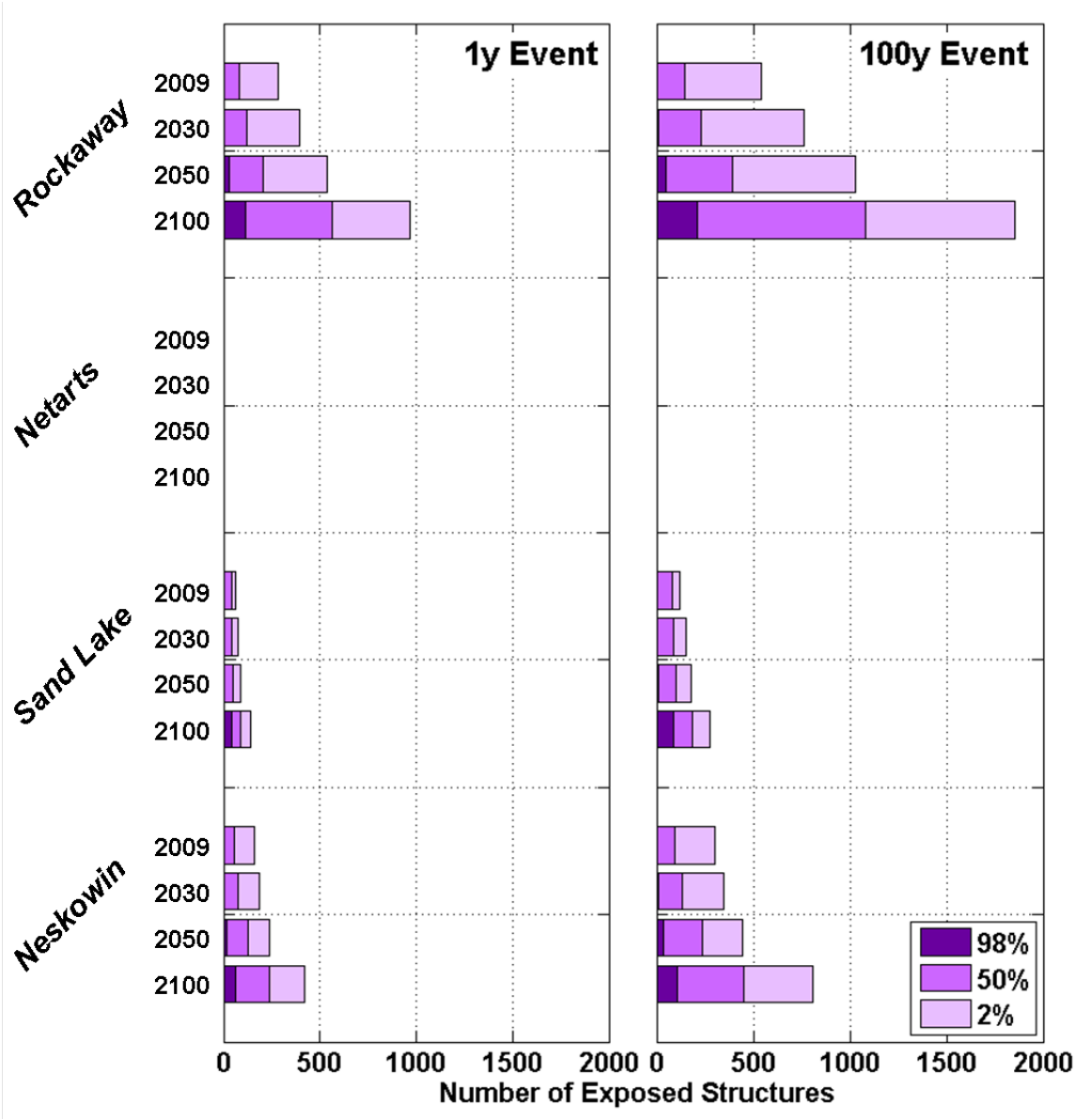

Figure 20. Number of structures within coastal change hazard zones through time for all littoral cells of Tillamook County associated with the 98%, 50%, and 2% exceedance probabilities. The medium and light purples (50% and 2% exceedance probabilities) indicate the 95% confidence interval for the number of structures likely to be impacted.

There are also many roads within the coastal hazard zones (Figure 21). In 2009, between 2.9 and 7.6 km of road within the Rockaway littoral cell have the potential to be impacted by coastal change associated with the 1% annual chance TWL event. The impacted length of road increases to 12.2 km in 2050, and by 2100, up to 25.9 km of road is within the 2% exceedance zone. The Neskowin littoral cell is the next highest to be impacted, ranging from 5 km in 2009 to 11.3 km in 2100. In Netarts, although there are not many large, permanent structures within the hazard zones, there are a few roads that run parallel to the shoreline and may potentially be impacted by coastal change very early in the century. The small community of Tierra Del Mar is located within the Sand Lake littoral cell, which will almost be entirely exposed to coastal change hazards by 2100.

In addition to direct impacts to coastal infrastructure, there is also potential for the breaching of barrier spits that protect coastal bays late in the 21st century, especially if a significant storm were to occur or if landward barrier migration does not keep up with the increased rate of SLR in the future. At its narrowest point, Netarts Spit is ~100 m across from the position of the present-day dune toe to Netarts Bay. A breach would allow for ocean saltwater inundation, causing significant changes to estuarine water quality and habitat.

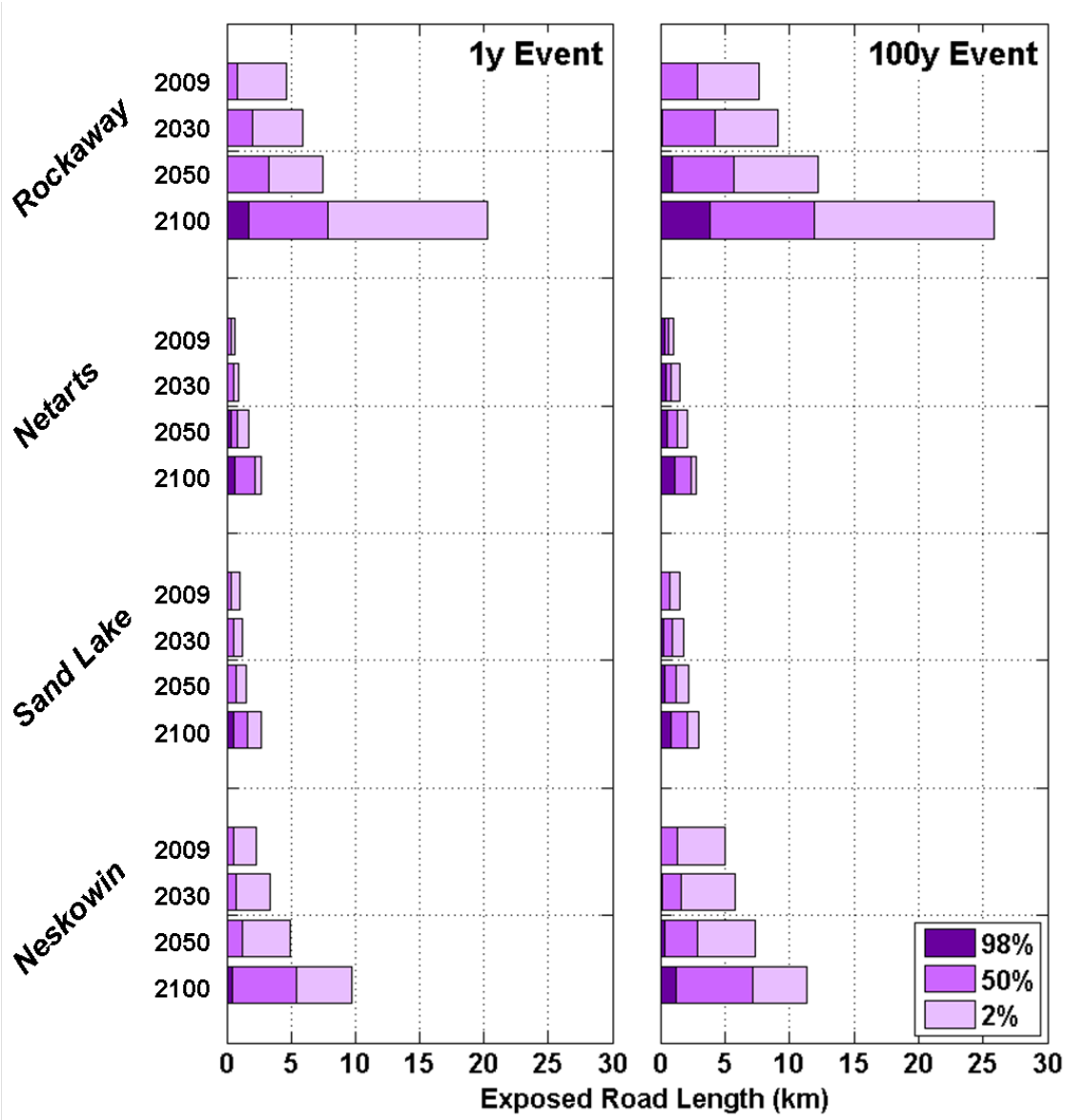

Figure 21. Length of road within coastal change hazard zones through time for all littoral cells of Tillamook County associated with the 98%, 50%, and 2% exceedance probabilities. The medium and light purples (50% and 2% exceedance probabilities) indicate the 95% confidence interval for the length of roads likely to be impacted.

5. DISCUSSION

The probabilistic approach to develop coastal change hazard zones described here allows the relative role of the various contributing factors to be explored. Below, the relative influence of climate and morphological variability in predicting erosion hazards is quantified. Next, is a brief comparison of the results with the existing Tillamook County coastal change hazard zones developed using a deterministic methodology by the Oregon Department of Geology and Mineral Industries (DOGAMI). Finally, various techniques that may improve the probabilistic approach – slated for future research – are discussed.

5.1 Relative Role of Varying Water Levels, Waves, and El Niños

The widths of the coastal change hazard zones developed are a function of a suite of climate change scenarios, involving various projections for future sea level, wave climate, and the frequency of occurrence of major El Niños. In order to understand the relative contribution of each of these components to the hazard zones, the impact of the individual 18 scenarios are isolated, using extreme TWLs in the Neskowin littoral cell in 2050 as an example. Table 5 quantifies the alongshore-averaged means and standard deviations computed based on the 100 morphological variability iterations for each of the 18 climate change scenarios. The standard deviations for each of the scenarios are quite small (< ~0.5 m), implying that there is minimal variability in the TWLs that result from the 100 different morphological configurations. As expected, the TWLs increase with increasing SLR and wave height projections, although they are only slightly higher (at least for the 100% annual chance TWL event) for the scenarios that involve a doubling in

the frequency of El Niño events (scenarios 1-9). By holding two of the three climate change components constant and comparing the extreme TWL values between the low and high projections of the third component, the relative impact of each one on the extreme TWLs can be analyzed. For example, to understand the impact of increasing wave height scenarios, the difference in the TWL values for scenarios 1 and 3 is calculated. The same can then be done for the SLR scenarios by comparing 1 and 7. Lastly, a comparison between 1 and 10 quantifies the variability in the El Niño scenarios. By finding the differences for all sets of projections in this manner and averaging the results, it is found that the variability in the TWL of the wave height scenarios has more of an impact on the extreme TWLs than does the variability in the SLR scenarios (0.4 m vs. 0.2 m, respectively). The difference in extreme TWLs for the El Niño scenarios is <0.1 m.

Table 6 shows the predicted erosion distances associated with each of the 18 climate change scenarios. The same trend is apparent for the total erosion predicted where the magnitude of erosion increases with increasing sea level and wave height projections. The total erosion distances range from 43.8 ± 22.9 m (59.1 ± 27.9 m) for the lowest scenario, 18 or LLM, to 66.1 ± 25.8 m (82.1 ± 29.7 m) for the highest scenario, 1 or HHH, for the 100% (1%) annual chance TWL events. By again holding two of the climate change components constant and varying the third, close examination of the individual scenarios reveals that the range of the SLR projections contributes more to the total magnitude of erosion than does the range of projections for wave climate, regardless of the time period of interest (Table 7) – the opposite result achieved for the impact on

extreme TWLs. The reason the smaller change in the TWL results in a bigger change in the estimated erosion for the SLR scenarios is that the SLR component of the TWLs are divided by the shallow shoreface slope, using the equation for $CC_{climate}$. In contrast, dividing the event component of the TWL by steeper backshore beach slopes, as is the case for CC_{event}, results in smaller erosion distances.

Table 5. Alongshore-averaged means and standard deviations for the 100% and 1% annual chance total water level (TWL) events in 2050 for each of the 18 climate change scenarios for the Neskowin littoral cell (n = 100 x the number of cross-shore profiles). The climate change scenarios are defined by their low (L), medium (M), and high (H) projections for SLR, wave heights, and El Niño frequency, in that order.

Climate Change Scenario		Annual Chance TWL Event (m)			
		100%		1%	
		mean	std	mean	std
1	HHH	6.4	0.42	7.4	0.52
2	HMH	6.2	0.40	7.2	0.50
3	HLH	6.0	0.38	7.0	0.48
4	MHH	6.3	0.42	7.2	0.52
5	MMH	6.1	0.40	7.0	0.50
6	MLH	5.9	0.38	6.8	0.48
7	LHH	6.2	0.42	7.1	0.52
8	LMH	6.1	0.40	6.9	0.50
9	LLH	5.9	0.38	6.7	0.48
10	HHM	6.3	0.42	7.4	0.50
11	HMM	6.2	0.40	7.2	0.48
12	HLM	6.0	0.37	7.0	0.46
13	MHM	6.2	0.42	7.2	0.51
14	MMM	6.1	0.40	7.0	0.49
15	MLM	5.9	0.37	6.8	0.47
16	LHM	6.2	0.42	7.1	0.51
17	LMM	6.0	0.39	6.9	0.49
18	LLM	5.8	0.37	6.7	0.47

Table 6. Alongshore-averaged means and standard deviations of erosion for each of the 18 climate change scenarios in 2050 for the Neskowin littoral cell (n = 100 x the number of cross-shore profiles).

Climate Change Scenario		$CC_{climate}$ (m)		CC_{event} (m)				Total Erosion Distance (m)			
				100% annual chance TWL event		1% annual chance TWL event		100% annual chance TWL event		1% annual chance TWL event	
		mean	std	mean	std	mean	std	mean	std	mean	std
1	HHH	26.3	2.4	39.7	25.3	55.8	29.2	66.1	25.8	82.1	29.7
2	HMH	26.3	2.4	36.7	24.3	51.8	28.5	63.2	24.7	78.1	29.0
3	HLH	26.3	2.4	33.9	23.2	48.0	27.7	60.4	23.6	74.4	28.2
4	MHH	16.6	1.5	39.7	25.3	55.6	29.2	56.4	25.6	72.2	29.5
5	MMH	16.6	1.5	36.8	24.3	51.7	28.5	53.6	24.6	68.4	28.8
6	MLH	16.6	1.5	33.9	23.2	48.0	27.6	50.7	23.4	64.7	27.9
7	LHH	10.8	1.0	39.8	25.4	55.4	29.1	50.7	25.5	66.2	29.3
8	LMH	10.8	1.0	36.7	24.3	51.7	28.5	47.6	24.4	62.5	28.7
9	LLH	10.8	1.0	33.9	23.2	48.0	27.7	44.8	23.3	58.9	27.8
10	HHM	26.3	2.4	38.5	24.9	56.3	29.5	65.0	25.3	82.6	30.0
11	HMM	26.3	2.4	35.6	23.8	52.4	28.8	62.1	24.2	78.7	29.3
12	HLM	26.3	2.4	32.7	22.7	48.7	27.9	59.3	23.1	75.1	28.4
13	MHM	16.6	1.5	38.6	24.9	55.8	29.3	55.3	25.2	72.5	29.6
14	MMM	16.6	1.5	35.6	23.8	52.0	28.6	52.4	24.1	68.7	29.0
15	MLM	16.6	1.5	32.8	22.8	48.3	27.8	49.6	23.0	65.0	28.1
16	LHM	10.8	1.0	38.6	24.9	55.7	29.3	49.4	25.1	66.5	29.5
17	LMM	10.8	1.0	35.7	23.9	51.8	28.5	46.6	24.0	62.6	28.7
18	LLM	10.8	1.0	32.8	22.8	48.2	27.8	43.8	22.9	59.1	27.9

Table 7. Impact of the SLR, wave climate, and El Niño scenario ranges on the total predicted erosion, expressed in terms of magnitude and percent increase from the lowest to highest projection when all other components are held constant.

TWL event	Year	Sea-level Rise		Wave Climate		El Niño Frequency	
		magnitude (m)	%	magnitude (m)	%	magnitude (m)	%
100% annual chance	2030	7.3	18	2.8	6	0.1	0
	2050	15.6	33	5.7	10	1.1	2
	2100	42.7	63	6.0	7	1.4	2
1% annual chance	2030	7.1	13	3.8	6	0	0
	2050	15.9	25	7.5	10	0	0
	2100	42.6	51	6.7	6	0	0

For example, scenarios involving the high SLR projection (1, 2, 3, 10, 11, and 12) result in 15.9 m of additional erosion, on average, associated with the 1% annual chance TWL event in 2050 over those involving the low SLR projection (7, 8, 9, 16, 17, and 18). This corresponds to a 25% increase in the magnitude of erosion between scenarios involving the low vs. high SLR projections when wave height and El Niño scenarios are held constant. For the same year and TWL event, the total erosion predicted for scenarios involving the high wave climate projection, where wave heights are allowed to increase through the year 2030 (1, 4, 7, 10, 13, and 16), is only 7.5 m greater (equivalent to a 10% increase) than the scenarios with the low projection where wave heights decrease over the same time period (3, 6, 9, 12, 15, and 18). Because the total predicted erosion increases significantly between 2050 and 2100 but the range in the wave height scenarios stays about the same (since wave heights were only allowed to increase until 2030), the relative percentage decreases over time.

Doubling the frequency of El Niño events in the future, however, does not have a significant impact on the width of the hazard zones. In fact, the magnitude of erosion predicted for the 100-year return TWL event is insensitive to a doubling in the frequency of El Niño, while the 1-year return TWL event only increases the total predicted erosion by 2%, at most. These results are surprising, but are possibly due to the fact that an increase in the water levels for only 2 out of 30 years is not affecting the calculation of extreme events, and therefore, the TWLs between the climate change scenarios with and without a doubling of El Niños are quite similar (refer back to Table 6).

5.2 Climate Uncertainty vs. Morphological Variability

To determine which is contributing more to the overall width of the coastal hazard zones, the relative influence of uncertainty associated with climate change and morphological variability is explored. Because the hazard zone width – or landward extent – is defined using the 95% confidence interval, this can be done by comparing the alongshore varying standard deviations of each. For one configuration of morphological parameters (i.e., the alongshore varying mean beach slope and dune toe elevation), the alongshore average standard deviation of the 18 climate change scenarios around the mean is found to be ~7.8 m (Figure 22). In contrast, the standard deviation of the set of 100 iterations of morphology around any given climate change scenario is ~18.3 m, on average, which is more than double that of the uncertainty due to climate alone. Figure 22 illustrates how the standard deviation of both components varies alongshore for the Neskowin littoral cell, and how they compare to the standard deviation of all 1800

erosion estimates combined. Based on these sensitivity analyses, morphological variability is more important than the uncertainty associated with the range of climate change scenarios applied here in determining the width of the coastal hazard zones. As statistical theory suggests, the total uncertainty (orange line in Figure 22) results from the quadrature addition of the climate (blue line) and morphological (green line) uncertainties.

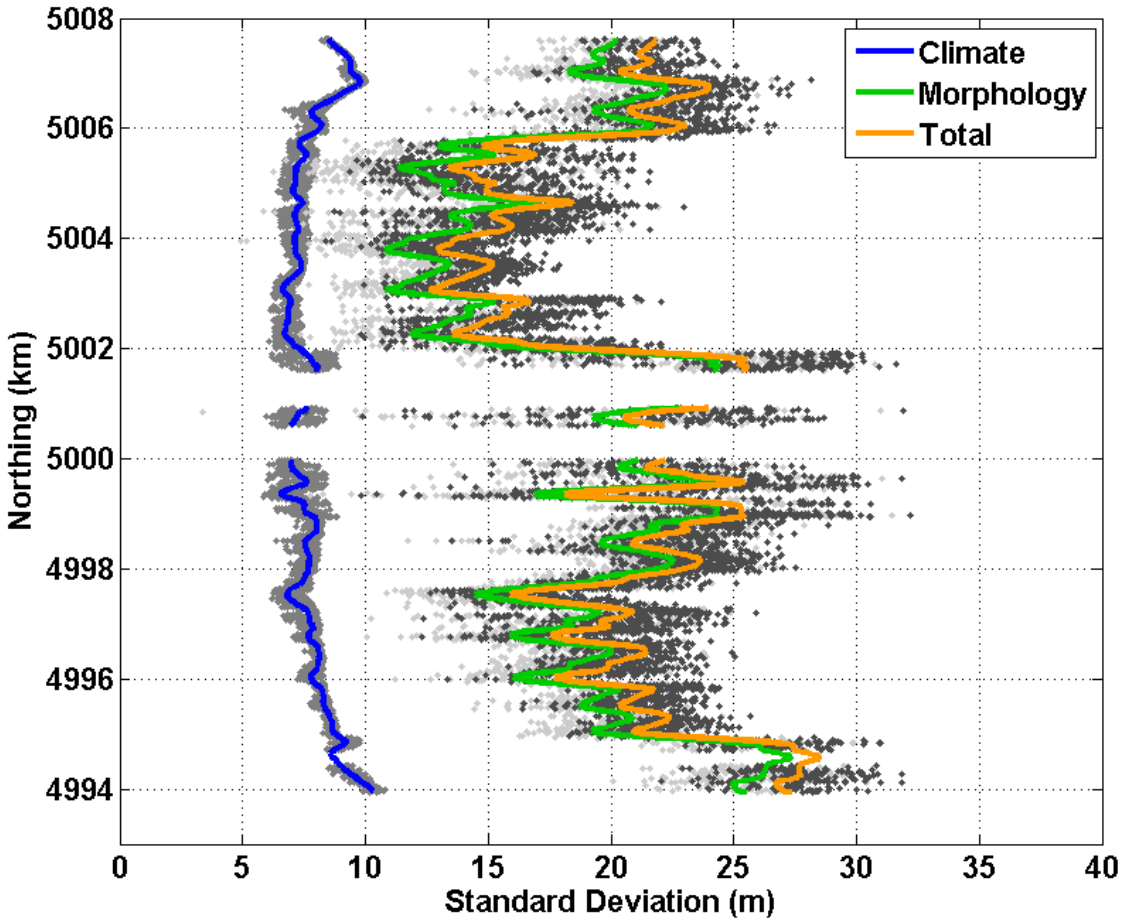

Figure 22. Variability due to climate (blue) vs. morphology (green) and the total variability of these uncertainties combined (orange) associated with the 100% annual chance TWL event in 2050 for the Neskowin littoral cell.

5.3 Sensitivity to Morphology

Since the beach slope is included in the calculations of CC_{event} in both the numerator, as expressed in the runup component of the TWL, and the denominator (Equation 8), the relationship between the expected erosion distance and a given dune toe elevation can vary significantly, as illustrated in Figure 23. For lower dune toe elevations, predicted dune erosion is negatively correlated to the backshore beach slope; flat beaches experience the most erosion. Conversely, for higher dune toes, the erosion distance is positively correlated to the backshore slope; more erosion occurs as the steepness of the beach increases. A flat beach with a high dune toe is likely to be a very wide beach where the horizontal component of the wave runup is not able to reach the dune toe as easily, so the potential for erosion is less. The combination of flat beach slopes and low dune toes that are characteristic of the southern ends of some littoral cells in Tillamook County puts communities located in these areas (e.g., Neskowin) in jeopardy as they are likely more vulnerable to coastal erosion during periods of elevated water levels.

The exact magnitude of expected erosion, however, depends on both the local geomorphology and the TWLs experienced. Figure 23 represents an example for a single condition of hydrodynamic inputs (wave height = 14.5 m, period = 17 s, measured tidal elevation = 4.3 m). For lower wave conditions, the positive dependence between slope and predicted erosion distance occurs at lower dune toe elevations than what is depicted for this example.

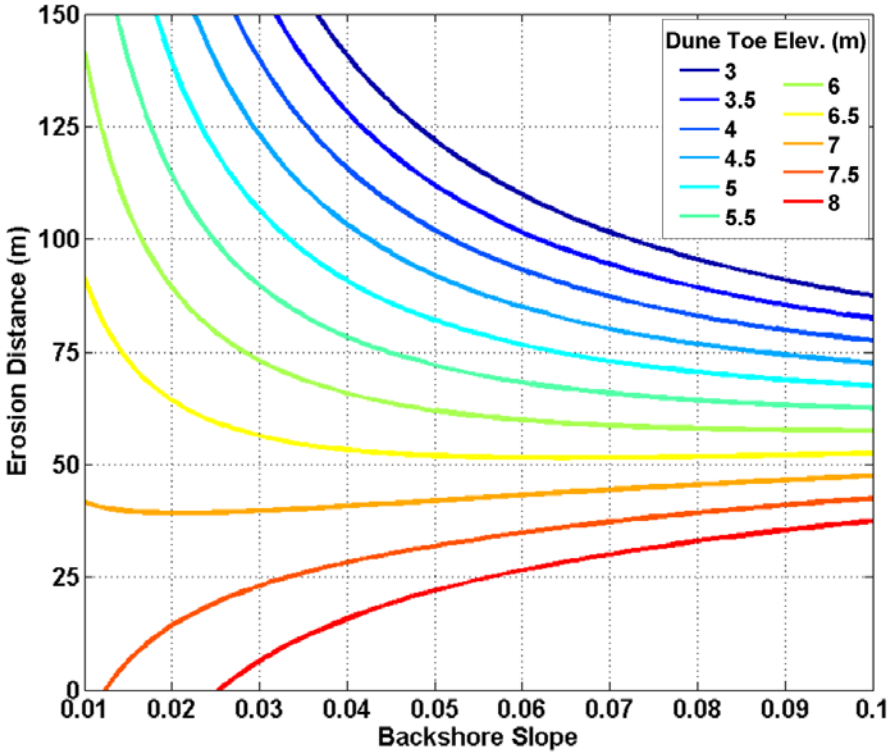

Figure 23. Sensitivity of K99 model to backshore beach slope and dune toe elevations, in meters, for one example of hydrodynamic inputs (wave height = 14.5 m, period = 17 s, measured tidal elevation = 4.3 m). Dune toe elevations increase downwards from 3 (dark blue) to 8 (red) m, by 0.5 m increments.

5.4 Comparing Results with Existing Deterministic Hazard Zones

There are many differences between the probabilistic approach developed here and the deterministic methods applied by Allan and Priest (2001) at DOGAMI used to create the existing coastal erosion hazard zones for the Oregon coast. While results from these two approaches are not directly comparable, it is interesting to examine where these conservative dune erosion predictions fall within the probabilistic estimates.

In contrast to the development of a TWL time series based on historical wave and water level data as done via the probabilistic approach developed in this thesis, Allan and

Priest (2001) defined a set of hydrodynamic variables that describe specific extreme storm events from which they calculate a single TWL associated with each event. The first event, or "high-risk," scenario is based on a large storm with wave heights on the order of 14.5 m occurring during an above average high tide. The "moderate-risk" scenario, which has a lower probability of occurrence, involves an even larger storm (wave heights ~16 m) and is coupled with 0.4 m of SLR estimated to occur over the next 100 years. Because these events are based on the worst storm in the wave record, the TWLs used in the deterministic approach are more extreme than the TWLs calculated from the probabilistic approach for either the 1-year or 100-year return level (Figure 24).

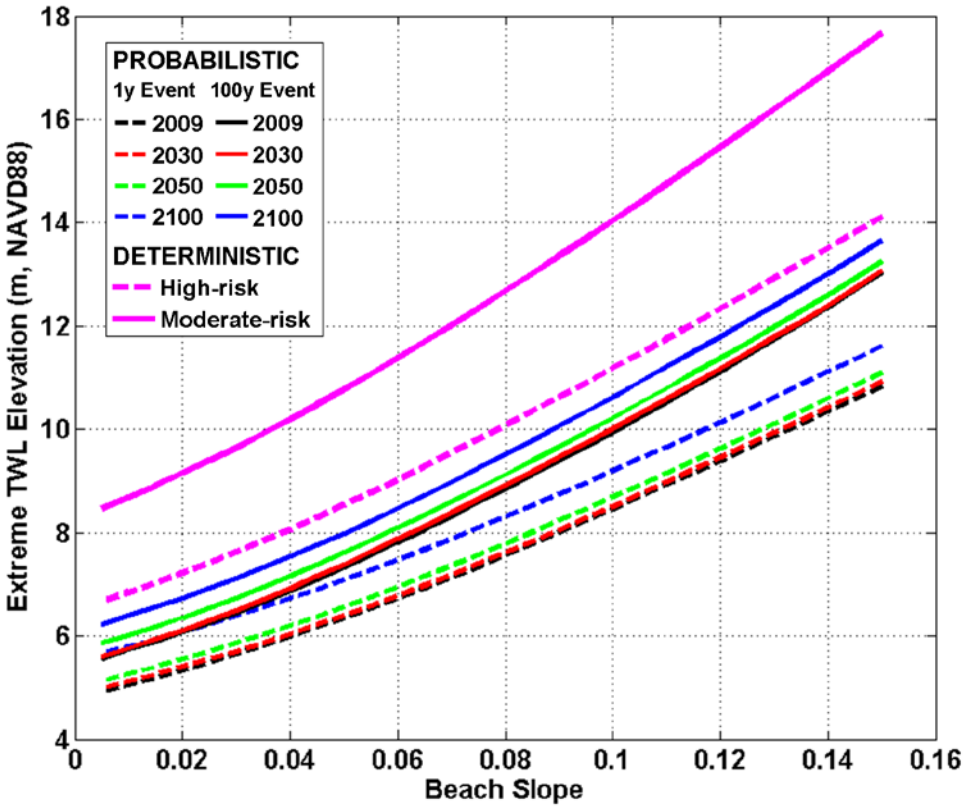

Figure 24. Difference in the total water levels (TWLs) between the mean values of the probabilistic approach and the deterministic methods by Allan and Priest (2001).

A key difference between the approach taken by DOGAMI and the methodology presented here is that the K99 dune erosion model is used to estimate the maximum potential erosion from the significant storm event plus SLR combined. By doing this, the rise in sea level is inaccurately being applied to features of the backshore rather than allowing the beach profile to move landward and upward as a function of the shoreface slope and then using the K99 model to estimate foredune erosion in response to an elevated TWL event.

The mean potential erosion distances for Tillamook County by Allan and Priest (2001) vary from ~80 m for their high-risk event to ~130 m associated with the moderate-risk event, depending on the littoral cell. To put this in the context of the probabilistic results, Figure 25 shows the alongshore-varying erosion distances for the high- and moderate-risk events compared to the probabilistically-defined mean and 95% confidence interval for erosion associated with the 1% annual chance TWL event in 2050, as applied to the Neskowin littoral cell. Erosion from the high-risk event is similar in magnitude to the mean erosion distances found using the probabilistic methodology in 2050 (on average, ~10 m greater), while the expected erosion associated with the moderate-risk event is ~23 m, on average, more than the 2% exceedance probability. The deterministic approach, however, imposes a fixed level of risk rather than providing coastal planners with a range of erosion probabilities so that they can decide the level of risk, the extremity of the event, and the time period of interest to them.

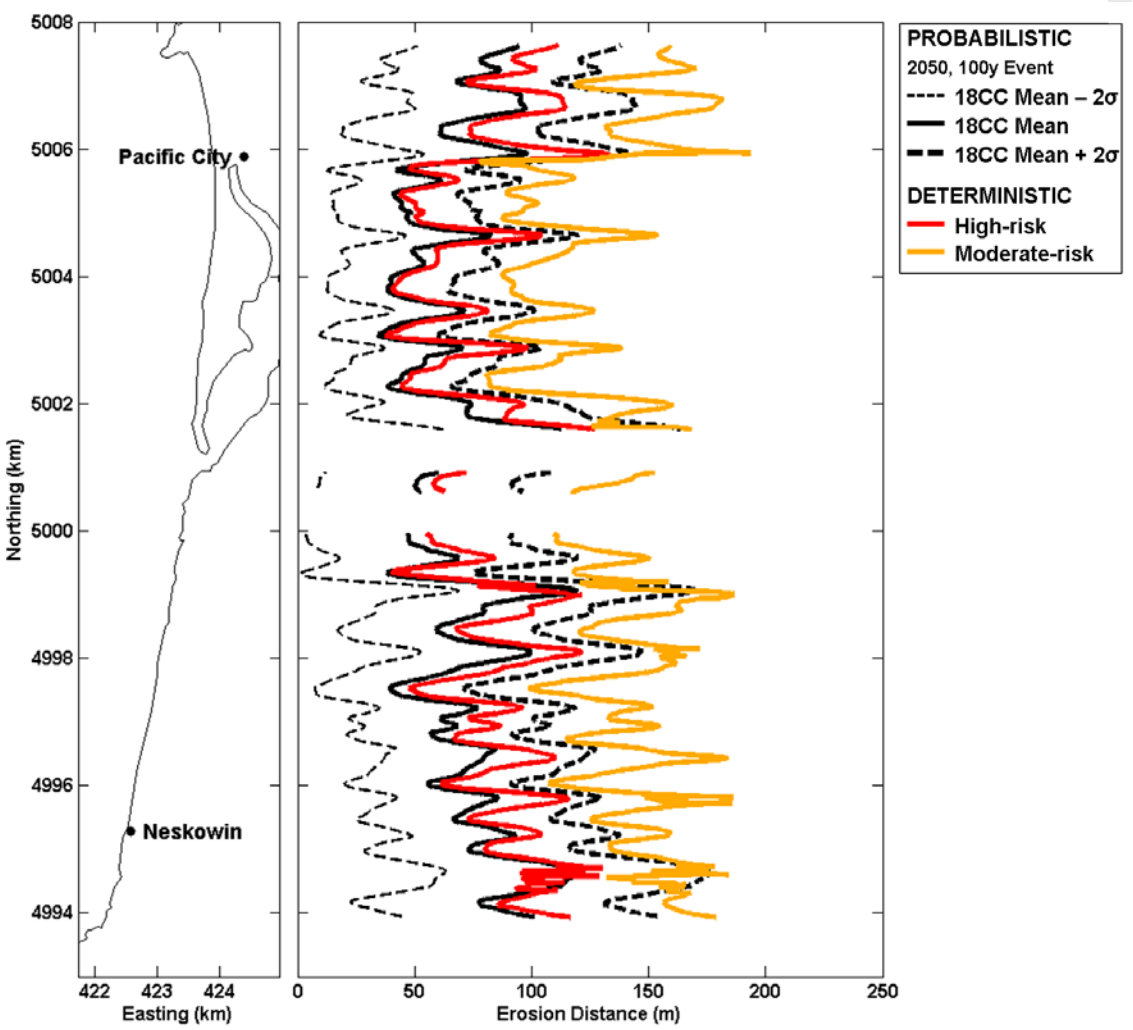

Figure 25. Difference in erosion distances between the probabilistic hazard zones for the 100-year return TWL event in 2050 vs. the deterministic zones by Allan and Priest (2001). Values are smoothed in the alongshore to remove variability less than 250 m.

5.5 Opportunities to Refine the Methodology

As stated previously, the approach presented here is designed to be modular. It can easily be modified to incorporate improved climate change inputs as they become available, such as new projections of SLR, wave climate, or a better understanding of the future variability in El Niño. The methodology can also accommodate more advanced

approaches for deriving climate change scenarios. For example, the output from general circulation models could be used to drive regional wave and flow models and develop alongshore varying extreme TWLs for a range of climate change scenarios.

Because of the way in which the extended TWL time series was calculated, there is inherent joint probability of waves and water levels occurring in the synthetic dataset. One way to modify the response-based, probabilistic approach would be to divide the historical TWL record into annual time series and then randomly append the datasets one year at a time until the desired length is reached. Another way to address this joint probability would be to run numerous simulations using the measured waves and non-tidal residuals so that the phasing and amplitudes of the predicted tides varied.

Furthermore, though simple coastal change models are used here, more sophisticated modeling approaches can be substituted where appropriate. For example, the K99 model is not process-based and does not include a term for time dependence. As an improvement, other event-scale coastal change models can be used if the necessary input data is available, such as the equilibrium dune erosion model of Kriebel and Dean (1993) or the wave impact model of Larsen et al. (2004) – see Mull (2010) for a comparison of these models with K99 as applied to the PNW. There are also simple ways to quantify the sediment budget-driven coastal change term in Equation 1, CC_{SB}, by projecting current shoreline change rates (Harris, 2011) or applying a one-line shoreline change model such as UNIBEST (WL|Delft Hydraulics, 1994).

5.6 Incorporation into the Tillamook County Erosion Hazards Adaptation Plan

Due to a growing need to address coastal hazards within the context of climate change and develop county-wide adaptation plans, Tillamook County, Oregon is currently drafting an Erosion Hazards Adaptation Framework Plan. This plan recommends that all coastal communities create a sub-plan specific to the local geomorphology and concerns of the community. The sub-plan for the community of Neskowin is already underway.

One of the greatest concerns of Neskowin is how their community will be impacted by coastal change and flooding hazards in light of a changing climate. Over the past few years, our group has been working closely with members of the Neskowin Coastal Hazards Committee and Tillamook County who have grown to support our research and wish to use the coastal change hazard zones as part of the scientific foundation for the Neskowin adaptation sub-plan. Per this request, a series of maps depicting future coastal change was provided to the Tillamook County coastal planner, as well as a series of exposure analyses specific for the community of Neskowin. A sample of the final hazard map product is shown in Figure 26, followed by exposure plots of homes, businesses, and roads within the hazard zones through time in Figure 27. The zones are presented in a slightly different manner than what was previously shown in this thesis, but they still represent the same information.

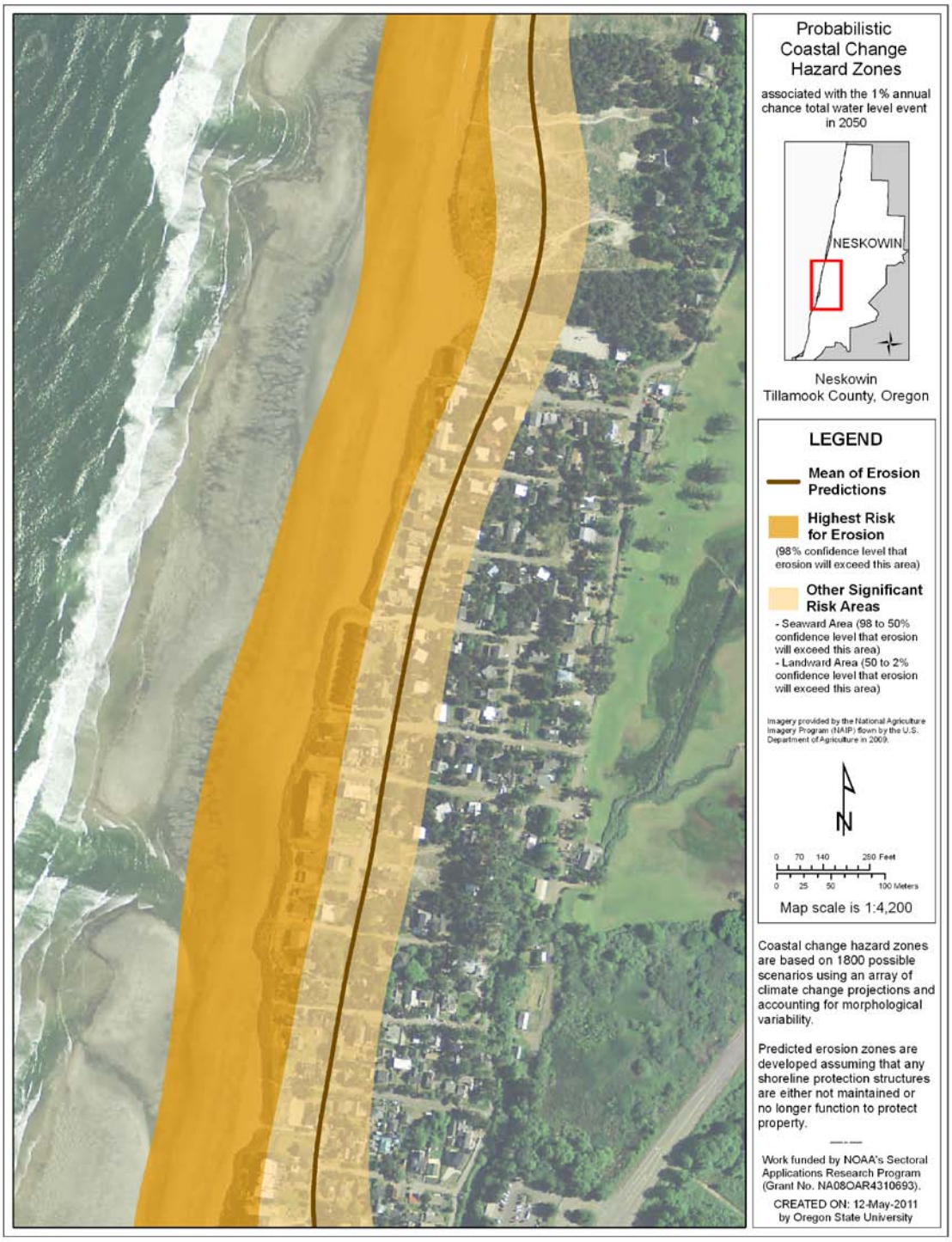

Figure 26. Example coastal change hazard zone map product developed for the Neskowin Erosion Hazard Adaptation Sub-Plan.

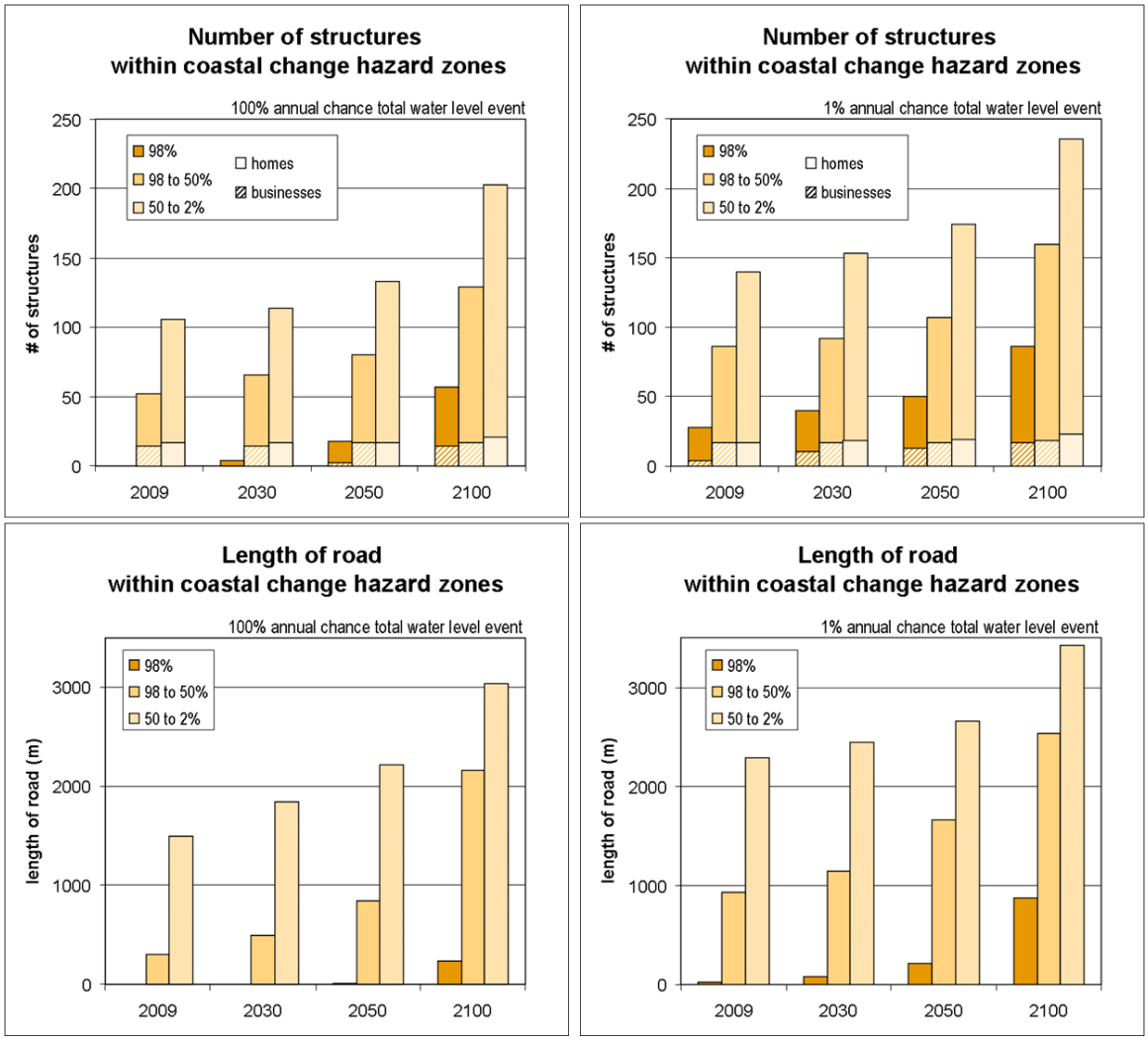

Figure 27. Exposure plots showing the potential impact of coastal change hazards to important community assets in Neskowin: number of structures (top) and length of road (bottom) for both the 100% (left) and 1% (right) annual chance TWL events. These plots were made to accompany the hazard zone map products shown in Figure 26.

6. CONCLUSIONS

The new, probabilistic methodology developed here can be used to quantify coastal change hazards and vulnerability for a variety of dune-backed beaches. The simplicity of the approach and its modular design allows for flexibility of input conditions and models used. By incorporating a wide range of projections for SLR, wave climate, and El Niño frequency, the uncertainty and variability associated with the impact of future climate change on TWLs and coastal erosion can be assessed, while simultaneously accounting for morphological variability. The results of coastal change models are then used to produce hazard zones that can be overlaid with various socioeconomic data in order to evaluate coastal vulnerability and community exposure. A probabilistic assessment of coastal change hazards is useful given the uncertainties associated with climate change and the dynamic nature of the coastal environment. In addition, rather than imposing one set of hazard zones on a local government, the approach presented here allows for decision-makers to choose the level of risk they are willing to accept as well as what time period and design event they would like to develop their planning documents for.

Here the methodology was applied to the Tillamook County coast in Oregon where a set of coastal change hazard zones of arbitrary confidence levels were developed for both the 100% and 1% annual chance TWL events at present (2009) and for years 2030, 2050, and 2100. Coastal change hazards are likely to increase in the future despite significant uncertainties associated with increasing sea levels, storminess, and El Niño frequency. As seen from the simple socioeconomic assessments conducted here,

exposure varies alongshore depending on land use within the coastal zone. The impact to coastal communities increases greatly in the latter half of the century, when SLR begins to play a larger part in shoreline retreat.

While the range of wave height scenarios applied here has a larger impact on the extreme TWLs than does the SLR scenarios, the range in SLR scenarios contributes more to the variability in total erosion than the wave height scenarios. The magnitude of estimated coastal change from both SLR and extreme events are significant; however, morphological variability contributes more to the overall variance and, hence, the width of the hazard zones. In order to most accurately portray the potential impacts of climate change on coastlines in the future, it is necessary to consider not only SLR but also changes in storminess and event-induced erosion which play a large role in the extreme TWLs experienced at the shoreline and often cause episodic erosion of protective foredunes.

The hazard map products developed and presented here, when combined with community vulnerability assessments, will provide science-based support to coastal communities and decision makers. As discussed earlier, the hazard zones are being incorporated into the new erosion hazards adaptation plan for Tillamook County. While it is encouraging that coastal communities are striving to protect and maintain their coastlines for future generations, it is still unclear how the products developed by this project will ultimately be used and whether or not they will successfully aid in local adaptation to climate change.

7. REFERENCES

Adger, W.N., 2006. Vulnerability. Global Environmental Change, 16, 268-281.

Allan, J.C. and P.D. Komar, 2000. Are ocean wave heights increasing in the eastern North Pacific? EOS, Transactions of the American Geophysical Union, 47, 561-567.

Allan and Komar, 2002. Extreme storms on the Pacific Northwest Coast during the 1997-98 El Niño and 1998-99 La Niña. Journal of Coastal Research, 18(1), 175-193.

Allan, J. C. and P.D. Komar, 2004. Environmentally compatible cobble berm and artificial dune for shore protection. Shore & Beach, 72(1), 9-18.

Allan, J. C. and P.D. Komar, 2006. Climate controls on U.S. West Coast erosion processes. Journal of Coastal Research, 22, 511-529.

Allan, J.C. and G.R. Priest, 2001. Evaluation of coastal erosion hazard zones along dune and bluff backed shorelines in Tillamook County, Oregon: Cascade Head to Cape Falcon Rep. Oregon Department of Geology and Mineral Industries, Open file report O-01-03, 126 pp.

Berkes, F., 2007. Understanding uncertainty and reducing vulnerability: Lessons from resilience thinking. Natural Hazards, 41, 283-295.

Bindoff, N.L., J. Willebrand, V. Artale, A, Cazenave, J. Gregory, S. Gulev, K. Hanawa, C. Le Quéré, S. Levitus, Y. Nojiri, C.K. Shum, L.D. Talley and A. Unnikrishnan, 2007. Observations: Oceanic Climate Change and Sea Level. In: Climate Change 2007: The Physical Science Basis. Contribution of Working Group I to the Fourth Assessment Report of the Intergovernmental Panel on Climate Change, [Solomon, S., D. Qin, M. Manning, Z. Chen, M. Marquis, K.B. Averyt, M. Tignor and H.L. Miller (eds)]. Cambridge University Press, Cambridge, United Kingdom and New York, NY, USA.

Bromirski, P.D., A.J. Miller, R.E. Flick, and G. Auad, in press. Dynamical suppression of sea level rise along the Pacific Coast of North America: Indications for imminent acceleration. Journal of Geophysical Research.

Bruun, P., 1962. Sea-level rise as a cause of shore erosion. Journal of the Waterways and Harbors Division, American Society of Civil Engineers, 88, 117-130.

Bruun, P., 1988. The Bruun Rule of erosion by sea-level rise: A discussion of large-scale two- and three-dimensional usages. Journal of Coastal Research, 4(4), 627-648.

Burgette, R.J., R.J. Weldon, and D. A. Schmidt, 2009. Interseismic uplift rates for western Oregon and along-strike variation in locking on the Cascadia subduction zone. Journal of Geophysical Research Letters, 114, B01408, 24 pp.

Callaghan, D.P., P. Nielsen, A. Short, R. Ranasinghe, 2008. Statistical simulation of wave climate and extreme beach erosion. Coastal Engineering, 55, 375-390.

Cazenave, A. and R.S. Nerem, 2004. Present-day sea level change: Observations and causes. Review of Geophysics, 42, RG3001, 20 pp.

Cazenave, A. and W. Llovel, 2010. Contemporary sea-level rise. Annual Review of Marine Science, 2, 145-173.

Church, J.A. and N.J. White, 2006. A 20th century acceleration in global sea-level rise. Geophysical Research Letters, 33, L01602, 4 pp.

Coles, S.G., 2001. An introduction to statistical modeling of extreme values. Springer, London, 208 pp.

Collins, M. and The CMIP Modelling Groups, 2005. El Niño- or La Niña-like climate change? Climate Dynamics, 24, 89-104.

Crossett, K.M., T.J. Culliton, P.C. Wiley, T.R. Goodspeed, 2004. Population trends along the coastal United States: 1980-2008. Coastal Trends Report Series, NOAA, National Ocean Service's Management and Budget Office, Special Projects, 54 pp.

Gornitz, V.M., T.W. Beaty, and R.C. Daniels, 1997. A coastal hazards data base for the U.S. West Coast. Oak Ridge, Tennessee: Oak Ridge National Laboratory, 162 pp.

Graham, N.E. and H.F. Diaz, 2001. Evidence for intensification of North Pacific winter cyclones since 1948. Bulletin of the American Meteorological Society, 82(9), 1869-1893.

Grinsted, A., J.C. Moore, and S. Jevrejeva, 2009. Reconstructing sea level from paleo and projected temperatures 200 to 2100 AD. Climate Dynamics, 34(4), 461-472.

Hammer-Klose, E. and R. Thieler, 2001. Coastal vulnerability to sea-level rise: A preliminary database for the U.S. Atlantic, Pacific and Gulf of Mexico coasts. Woods Hole, MA: United States Geological Survey (USGS).

Harris, E.L., 2011. Assessing physical vulnerability of the coast in light of a changing climate: An integrated, multi-hazard, multi-timescale approach. Master of Science thesis, Oregon State University, 91 pp.

Heberger, M., H. Cooley, P. Herrera, P.H. Gleick, and E. Moore of the Pacific Institute, 2009. The impacts of sea-level rise on the California coast. CEC-500-2009-024-F, 115 pp.

Hegerl, G.C., F. W. Zwiers, P. Braconnot, N.P. Gillett, Y. Luo, J.A. Marengo Orsini, N. Nicholls, J.E. Penner and P.A. Stott, 2007. Understanding and Attributing Climate Change. In: Climate Change 2007: The Physical Science Basis. Contribution of Working Group I to the Fourth Assessment Report of the Intergovernmental Panel on Climate Change, [Solomon, S., D. Qin, M. Manning, Z. Chen, M. Marquis, K.B. Averyt, M. Tignor and H.L. Miller (eds)]. Cambridge University Press, Cambridge, United Kingdom and New York, NY, USA.

Holgate, S. J., 2007. On the decadal rates of sea level change during the twentieth century. Geophysical Research Letters, 34, L01602, 4 pp.

Horton, R., C. Herweijer, C. Rosenzweig, J. Liu, V. Gornitz, and A.C. Ruane, 2008. Sea level rise projections for current generation CGCMs based on the semi-empirical method. Geophysical Research Letters, 35, L02715, 5 pp.

Jevrejeva, S., J.C. Moore, and A. Grinsted, 2010. How will sea level respond to changes in natural and anthropogenic forcings by 2100? Geophysical Research Letters, 37, L07703, 5 pp.

Kaminsky, G.M., Ruggiero, P., and Gelfenbaum, G., 1998. Monitoring coastal change in southwest Washington and northwest Oregon during the 1997/98 El Niño. Shore and Beach, 66(3), 42-51.

Komar, P.D., 1986. The 1982-83 El Niño and erosion on the coast of Oregon. Shore and Beach, 54, 3-12.

Komar, P.D., 1998. The Pacific Northwest Coast: Living with the shores of Oregon and Washington. Duke University Press, 195 pp.

Komar, P.D., J.C. Allan, and P. Ruggiero, in press. Sea level variations along the U.S. Pacific Northwest coast: Tectonic and climate controls. Journal of Coastal Research.

Komar, P.D., W.G. McDougal, J.J. Marra, and P. Ruggiero, 1999. The rational analysis of setback distances: Applications to the Oregon Coast. Shore and Beach, 67, 41-49.

Kriebel, D.L. and R.G. Dean, 1993. Convolution method for time-dependent beach-profile response. Journal of Waterway, Port, and Coastal Engineering, 119, 204-226.

Kumar, T.S., R.S. Mahendra, S. Nayak, K. Radhakrishnan, and K.C. Sahu, 2010. Coastal vulnerability assessment for Orissa State, east coast of India. Journal of Coastal Research, 26(3), 523–534.

Larson, M., L. Erikson, and H. Hanson, 2004. An analytical model to predict dune erosion due to wave impact. Coastal Engineering, 51, 675-696.

Leuliette, E.W., R.S. Nerem, and G.T. Mitchum, 2004. Calibration of TOPEX/Poseidon and Jason altimeter data to construct a continuous record of mean sea level change. Marine Geodesy, 27(1-2), 79-94.

Mazzotti, S., C. Jones, and R.E. Thomson, 2008. Relative and absolute sea level rise in western Canada and northwestern United States from a combined tide gauge-GPS analysis. Journal of Geophysical Research, 113, C11019, 19 pp.

Meehl, G.A., T.F. Stocker, W.D. Collins, P. Friedlingstein, A.T. Gaye, J.M. Gregory, A. Kitoh, R. Knutti, J.M. Murphy, A. Noda, S.C.B. Raper, I.G. Watterson, A.J. Weaver and Z.-C. Zhao, 2007. Global Climate Projections. In: Climate Change 2007: The Physical Science Basis. Contribution of Working Group I to the Fourth Assessment Report of the Intergovernmental Panel on Climate Change, [Solomon, S., D. Qin, M. Manning, Z. Chen, M. Marquis, K.B. Averyt, M. Tignor and H.L. Miller (eds)]. Cambridge University Press, Cambridge, United Kingdom and New York, NY, USA.

Méndez, F.J., Menéndez, M., Luceño, A., Losada, I.J., 2006. Estimation of the long-term variability of extreme significant wave height using a time-dependent peak over threshold (POT) model. Journal of Geophysical Research 111, C07024, 13 pp.

Mull, J.M., 2010. Coastal sand dunes in the U.S. Pacific Northwest: Regional variability in foredune geomorphology and associated physical vulnerability to hazards. Master of Ocean Engineering thesis, Oregon State University, 134 pp.

Nakicenovic, N., J. Alcamo, G. Davis, B. de Vries, J. Fenhann, S. Gaffin, K. Gregory, A. Grubler, T.Y. Jung, T. Kram, E.L. La Rovere, L. Michaelis, S. Mori, T. Morita, W. Pepper, H. Pitcher, L. Price, K. Riahi, A. Roehrl, H.H. Rogner, A. Sankovski, M. Schlesinger, P. Shukla, S. Smith, R. Swart, S. van Rooijen, N. Victor, and Z. Dadi, 2000. Special Report on Emissions Scenarios: A Special Report of Working Group III of the Intergovernmental Panel on Climate Change, N. Nakicenovic and R. Swart (eds). Cambridge University Press, Cambridge, United Kingdom, 570 pp.

NOAA Center for Tsunami Research, 2004. Central Oregon, OR 6 arc-second MHW Tsunami Inundation DEM. NOAA's National Geodetic Data Center (NGDC), retrieved 18-Nov-10, available online at: http://www.ngdc.noaa.gov/mgg/inundation/.

NOAA Coastal Services Center, 2002. 2002 NASA/USGS Airborne LiDAR Assessment of Coastal Erosion (ALACE) Project for California, Oregon, and Washington Coastlines. NOAA's Ocean Service, Coastal Services Center (CSC), available online at: http://www.csc.noaa.gov/ldart.

Oregon Climate Change Research Institute (OCCRI), 2010. Oregon Climate Assessment Report, K.D. Dello and P.W. Mote (eds). College of Oceanic and Atmospheric Sciences, Oregon State University, Corvallis, OR, 473 pp. available online at: www.occri.net/OCAR.

Pfeffer, W.T., J.T. Harper, and S. O'Neel, 2008. Kinematic constraints on glacier contributions to 21st-century sea-level rise. Science, 321, 1340-1343.

Philip Williams & Associates, Ltd., 2009. California coastal erosion response to sea level rise – Analysis and mapping. San Francisco, California, 65 pp.

Plant, N.G., K.T. Holland, and J.A. Puelo, 2002. Analysis of the scale of errors in nearshore bathymetric data. Marine Geology, 191, 71-86.

Rahmstorf, S., 2007. A semi-empirical approach to projecting future sea-level rise. Science, 315, 368-370.

Rahmstorf, S., 2010. A new view on sea level rise. Nature, 4, 44-45.

Rajagopalan, B., U. Lall, and M.A. Cane, 1997. Anomalous ENSO occurrences: An alternative view. Journal of Climate, 10, 2351-2357.

Revell, D.L., R. Battalio, B. Spear, P. Ruggiero, and J. Vandever, in press. A methodology for predicting future coastal hazards due to sea-level rise on the California coast. Climatic Change.

Ruggiero, P., G.M. Kaminsky, G. Gelfenbaum, and B. Voigt, 2005. Seasonal to interannual morphodynamics along a high-energy dissipative littoral cell. Journal of Coastal Research, 21(3), 553-578.

Ruggiero, P., P.D. Komar, J.C. Allan, 2010. Increasing wave heights and extreme value projections: The wave climate of the U.S. Pacific Northwest. Coastal Engineering, 57(5), 539-552.

Ruggiero, P., P.D. Komar, W.G. McDougal, W.G. and R.A. Beach, 1996. Extreme water levels, wave runup, and coastal erosion. Proceedings of the 25th Coastal Engineering Conference, ASCE, 2793-2805.

Ruggiero, P., P.D. Komar, W.G. McDougal, J.J. Marra, and R.A. Beach, 2001. Wave runup, extreme water levels, and the erosion of properties backing beaches. Journal of Coastal Research, 17, 407-419.

Ruggiero, P. and J.H. List, 2009. Improving accuracy and statistical reliability of shoreline position and change rate estimates. Journal of Coastal Research, 25(5), 1069-1081.

Shaw, J., R.B. Taylor, S. Solomon, H.A. Christian, and D.L. Forbes, 1998. Potential impacts of global sea-level rise on Canadian coasts. The Canadian Geographer, 42(4), 365-379.

Stockdon, H.F., R.A. Holman, P.A. Howd, and A.H. Sallenger, Jr., 2006. Empirical parameterization of setup, swash, and runup. Coastal Engineering, 53, 573-588.

Stockdon, H.F., K.S. Doran, and A.H. Sallenger, Jr., 2009. Extraction of LiDAR-based dune crest elevations for use in examining the vulnerability to beaches during inundation during hurricanes. Journal of Coastal Research, 53, 59-65.

Thieler, E.R., and Hammar-Klose, E.S., 1999, National assessment of coastal vulnerability to sea-level rise, U.S. Atlantic coast: U.S. Geological Survey, Open-File Report 99-593, 1 sheet.

Trenberth, K.E. and T.J. Hoar, 1997. El Niño and climate change. Geophysical Research Letters, 24(23), 3057-3060.

Turner, B.L., R.E. Kasperson, P.A. Matson, J.J., McCarthy, R.W. Corell, L. Christensen, N. Eckley, J.X. Kasperson, A. Luers, M.L. Martello, C. Polsky, A. Pulsipher, and A. Schiller, 2003. A framework for vulnerability analysis in sustainability science. Proceedings of the National Academy of Sciences, 100(14), 8074-8079.

University of Colorado Sea Level Change group, 2010. “Univ of Colorado 2010_rel3” retrieved 18-Aug-10, available online at: http://sealevel.colorado.edu/index.php.

van Oldenborgh, G.J., S.Y. Philip, and M. Collins, 2005. El Niño in a changing climate: a multi-model study. Ocean Science, 1, 81-95.

Vermeer, M., and S. Rahmstorf, (2009), Global sea level linked to global temperature. Proceedings of the National Academy of Sciences of the United States of America, 106(51), 21527-21532.

WL|Delft Hydraulics, 1994. UNIBEST, a software suite for the simulation of sediment transport processes and related morphodynamics of beach profiles and coastline evolution. Programme manual, WL|Delft Hydraulics, Delft, The Netherlands, pp 39.

Wood, N., 2007. Variations in community exposure and sensitivity to tsunami hazards in Oregon. USGS Scientific Investigations Report 2007-5283, United States Geological Survey, Reston, VA, 43 pp.

Wright, L.D. and A.D. Short, 1983. Morphodynamics of beaches and surf zones in Australia. In: Handbook of Coastal Processes and Erosion, P.D. Komar (ed.), CRC Press, Boca Raton, FL, 35–64.

Wunsch, C., R.M. Ponte, and P. Heimbach, 2007. Decadal trends in sea level patterns: 1993-2004. Journal of Climate, 20, 5889-5911.